DSTO

# Application of Detection Theory to the Measurement of the Minimum Detectable Signal for a Sinusoid in Gaussian Noise Displayed on a Lofargram

A. Grigorakis

DSTO-TR-0568



DEPARTMENT ◆ OF DEFENCE

DEFENCE SCIENCE AND TECHNOLOGY ORGANISATION

# Application of Detection Theory to the Measurement of the Minimum Detectable Signal for a Sinusoid in Gaussian Noise Displayed on a Lofargram

*A. Grigorakis*

**Maritime Operations Division**
**Aeronautical and Maritime Research Laboratory**

DSTO-TR-0568

## ABSTRACT

A review of detection threshold concepts is followed by an investigation into published theory for the detection of signals in noise. A set of empirical formulae relating minimum detectable signal to some basic sonar system parameters is presented. The formulae are compared and a recommendation made as to which is the most useful for the calculation of an omnidirectional narrowband lofargram minimum detectable signal for power detection of sinusoidal signals in Gaussian noise.



DEPARTMENT OF DEFENCE

DEFENCE SCIENCE AND TECHNOLOGY ORGANISATION

*Published by*

*DSTO Aeronautical and Maritime Research Laboratory*
*PO Box 4331*
*Melbourne Victoria 3001 Australia*

*Telephone: (03) 9626 7000*
*Fax: (03) 9626 7999*

*AR-010-148*
*August 1997*

**APPROVED FOR PUBLIC RELEASE**

# Application of Detection Theory to the Measurement of the Minimum Detectable Signal for a Sinusoid in Gaussian Noise Displayed on a Lofargram

## Executive Summary

This report supports the development of tools for the measurement of sonobuoy acoustic processor performance. It contains a review of detection threshold concepts and an investigation into the published literature relating to the detection of signals in noise. The tutorial style coverage of the detection of sinusoids in noise using lofargrams provides an introduction to those involved in signal analysis, acoustic processor testing and the training of sonar operators.

Minimum detectable signal (MDS) studies are of interest because they provide the ability to quantify the performance of systems designed to detect a signal in a background of noise. Absolute performance can be compared to the theoretical ideal, while relative performance can be used to quantify the effect of changes to system hardware or software.

Study of the literature shows several analysts have tackled and solved much of the more difficult detection theory, (to an accuracy of tenths of a decibel), with a high degree of consistency between analysts. This paper puts that work into a context suitable for sonar system detection performance studies.

Practical spectrogram and lofargram processing and display limitations are then discussed, and an attempt made to quantify their effect upon a systems MDS.

# Author

**A. Grigorakis**
Maritime Operations Division

*Mr. Grigorakis was born in Adelaide, South Australia in 1958. The University of Adelaide awarded him a B.Sc. in 1980 and a B.E.(Electrical, Honours) in 1981. He has been with DSTO for 15 years. During that time he has worked in radio frequency communications, switching and networks, fibre optics, interactive graphics, digital signal processing, new sonobuoy systems and, recently, airborne sonar.*

# Contents

# 1. Introduction

This report describes work carried out in support of Tasks ADA 95/161 'Support for P3-C Airborne Acoustic Systems' sponsored by Director General Force Development (Aerospace) and NAV 95/160 'Support for S-70B-2 Airborne Acoustic Systems', sponsored by Director Naval Warfare.

The aim of this work was to review in detail the published literature on detection threshold theory as it applies to the detection of sonar signals in a background of noise.

Radar technology appears to have provided the initial motivation for extensive development of the theory of detection of signals in noise, but similar problems also soon arose in sonar, resulting in a large body of related theoretical studies.

Detection theory has a long history, as seen from [1 Lawson and Uhlenbeck], [2 Harrington], [3 Reich and Swerling], [4 Peterson et al.], [5 Helmstrom], [6 Marcum] and [7 Whalen], with considerable analytic effort having being applied to models of the detection process, ranging from the detection of unknown (and noise like) signals in noise to the detection of sinusoidal signals of known frequency, phase and amplitude in noise. The input noise, in most studies, has been assumed to be Gaussian for mathematical simplicity.

Equations describing the detection process have usually not been solvable in closed form. However, several analysts such as [8 Marcum], [9 Robertson] and [10 Nuttall ], have applied numerical techniques and simplifying approximations, for particular signal and noise conditions, to arrive at useful solutions. Further, in recent times a closed form curve fitted approximation to the [9 Robertson] solutions has been developed by [11 Albersheim].

By selecting and interpreting appropriate analyses, this report aims to apply the numerical results of relevant theory to detection threshold estimation for the case of sinusoidal signals of random phase in Gaussian noise, examined on a sonar system's lofargram display.

# 2. Definitions

To clarify the nomenclature used in this report, and introduce some frequently used terms and abbreviations, the following definitions are presented. They may not be universal to all authors, but are widely accepted.

## 2.1 Detection Threshold (*DT*)

*DT* is defined as the Signal to Noise Ratio (*SNR*), at the systems receiver input, required to achieve detection of a signal in noise with a specified Probability of Detection ($P_d$) and a specified Probability of False Alarm ($P_{fa}$). This report shall use a convention of $P_d = 0.5$ (50%) and $P_{fa} = 10^{-4}$ (0.01%), as these represent useful operational sonar parameters.

## 2.2 Minimum Detectable Signal (*MDS*)

*MDS* is closely related to *DT* and is used to quantify the overall performance of sonar systems. It is defined as the Signal to Noise Ratio (*SNR*), at the systems sensor input, required to achieve detection of a signal in noise at the final output, with a specified Probability of Detection ($P_d$) and a specified Probability of False Alarm ($P_{fa}$). *MDS* is therefore inclusive of any beamforming processing by the system. Note that in an omnidirectional sonobuoy system, if the hydrophone, radio transmission system and signal conditioning are loss free, *MDS* = *DT*.

## 2.3 Power Spectrum and Power Spectral Density (*PSD* or *psd*)

The total power $P_x$ of a signal $x(t)$, (in the sense of being related to physical power by a dimensionless scaling constant) is, from [16 Press, p.498] and Parseval's Theorem,

$$P_x = \int_{-\infty}^{\infty} |x(t)|^2 \, dt = \int_{-\infty}^{\infty} |X(f)|^2 \, dt \qquad (4)$$

if the Fourier transform $X(f)$ of $x(t)$ exists. The quantity $|X(f)|^2$ is known as the power spectrum of the signal $x(t)$, and is real. Power spectral density (*psd*) is obtained by dividing $|X(f)|^2$ by the analysis filter bandwidth [41 Randall p.142 and 32]. The result has units of Volts$^2$seconds/Hertz, and is independant of frequency.

It is necessary to identify two classes of signal - stationary deterministic (e.g. sinusoids) and stationary stochastic (i.e. random) . A sinusoidal signal component has a Fourier term which is a delta function, zero width and infinite height, but finite area defined by the power of the sinusoid. Hence the *psd* of a discrete frequency is meaningless because it has zero bandwidth. Conversely, a random signal *psd* must be integrated over a finite bandwidth to give a finite energy. In detection theory, we deal with sinusoids in noise, analysed with a defined bandwidth *B*.

A continuous signal $x(t)$ which represents a stationary process could theoretically have infinite power, as it exists for all time. This means the Fourier integral over all time is unbounded and therefore the signal would not have a Fourier transform. It does,

however, have finite average energy, and therefore can have a power spectrum: this is also known as an envelope spectrum [17 Hodgekiss and Anderson, p.215]. To deal with such signals a finite sample over $2T_0$ seconds is taken for analysis, where $T_0$ is an arbitrary value. The actual power spectrum is then the expected value [15 Proakis p.870] of

$$P_x(f) = \frac{1}{2T_0}\left|\int_{-T_0}^{T_0} x(t)e^{-j2\pi ft}dt\right|^2 \tag{5}$$

as the blocked time interval $T_0 \to \infty$ [15 Proakis, p.870].

If $x(t)$ is a real signal, then the one sided power spectrum (incorporating both positive and negative frequencies) is

$$P_x(f) = |X(f)|^2 + |X(-f)|^2, \qquad 0 \le f < \infty \tag{6}$$

or

$$P_x(f) = 2|X(f)|^2, \qquad 0 \le f < \infty. \tag{7}$$

## 2.4 Periodogram

A display of power spectral density or frequency spectrum, (which may include the average of many independent measurements) is known as a periodogram [15 Proakis, p.869] and [16 Press, p.574], or sometimes a spectrogram. A biased psd estimate, in the sense that it is not a consistent estimate of the true power density spectrum (see section 4.1), of a time series $x(n)$ is given by the periodogram $psd_x(f_n)$ [15 Proakis, p.872] where

$$psd_x(f_n) = \frac{1}{NB}\left|\sum_{n=0}^{N-1} x(n)e^{-j2\pi fn}\right|^2. \tag{3}$$

Note that the DFT bin width $B$ has been included in Equation (3). Many texts use terms such as 'power density spectrum' and 'power spectral density' without applying the necessary frequency scaling to the expressions. This does not affect the shape of the resulting spectrum, only the scaling and units. Figure 1 is an example of a DFT generated periodogram, with a smooth line joining each value to produce a continuous displayed result. Decibel scaling is produced by calculating $10\log_{10}(P_x(f))$.

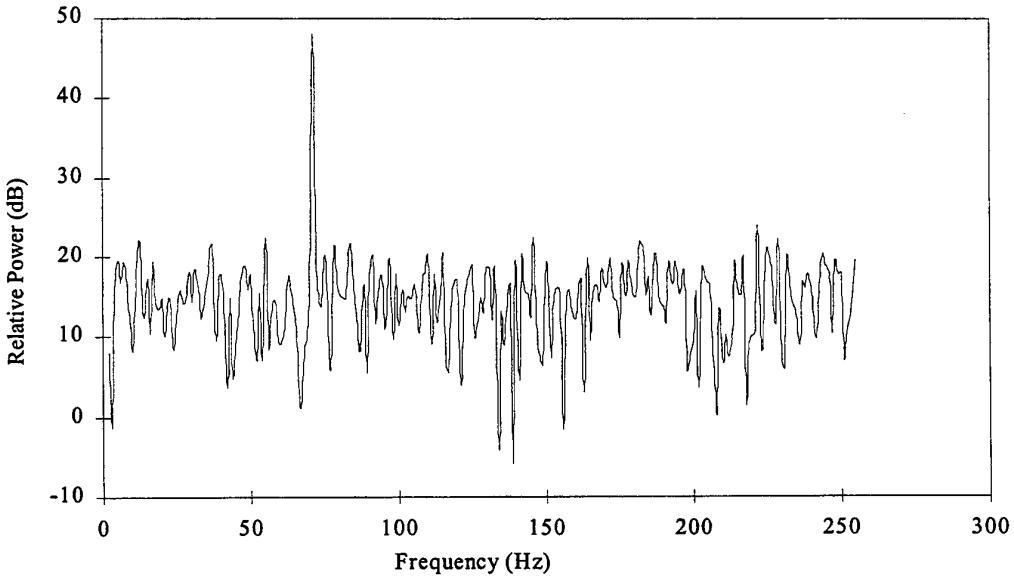


*Figure 1. A periodogram showing a sinusoid in noise.*

When the magnitude of a windowed (and possibly overlap processed) Fast Fourier Transform is used, the displayed result is sometimes referred to as a Welch periodogram [15 Proakis, p.877] and [14 Nielsen, p.73], and is often found in sonar signal processing.

The variance of a periodogram estimate of the power spectral density does not approach zero as the number of samples (or block size) is increased [18 Marple, p.127]. To this extent, a periodogram can be considered a biased estimator of the true *psd*. An average of several independent periodograms (for example, Bartlett's smoothing procedure [15 Proakis p.875] and [18 Marple, p.153]) is required to obtain an estimate whose variance does approach zero [19 Leon-Garcia, p.422].

## 2.5 LOFARgram

LOFAR (or lofar) is an acronym, from early sonar, for LOw Frequency Analysis and Recording. A lofargram is a display, often used to show sonar data, which plots time versus frequency with intensity a function of energy level. It usually comprises a vertically scrolling time history of intensity modulated lines (or rows) which represent consecutive frequency spectra (spectrograms) of a continuous input signal: an example is Figure 2. It may be visualised as a column of two dimensional periodograms, where brighter points indicate a stronger signal in that time interval (or row) and frequency interval (or column). Each row comprises pixels, where the intensity of each pixel represents the energy in a small frequency window (or bin) over a particular period of time. Columns represent sequential frequency intervals and rows represent consecutive time intervals.

Lofargrams assist an observer using pattern recognition to visually identify continuous narrowband signal frequencies, apparent as vertical lines, as the spectral contribution will statistically place more energy in those spectral bins corresponding to the presence of a narrowband signal.

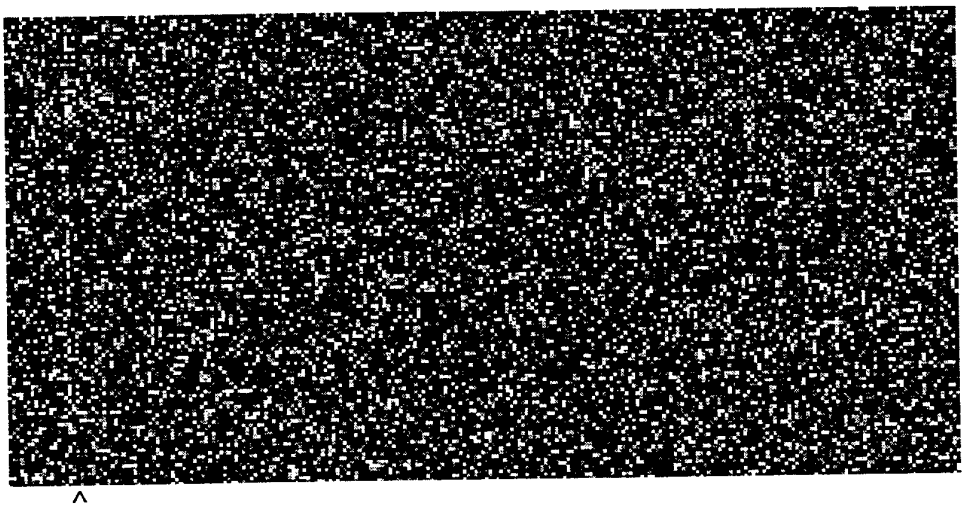

^

Note presence of a sinusoidal tone at this frequency.

*Figure 2. A lofargram display. The vertical axis is time and the horizontal axis frequency.*

Usually each display row is the result of coherent bandpass filtering, (via a windowed Discrete Fourier Transform), and subsequent incoherent filtering (column based energy summation). Incoherent summation may also be described as post detector integration.

## 2.6 Equivalent Noise Bandwidth (*ENBW*, $B_n$)

When a time domain signal is windowed (see Section 4.1.2), there is a complementary effect in the frequency domain. One measure of this is the *ENBW*, the bandwidth of a rectangular filter with the same centre frequency which would pass an equivalent amount of noise. Thus if a receiving system has a frequency response $H(f)$ then, according to [12 Meyer and Mayer, p. 3]

$$B_n = \frac{1}{|H(f_0)|^2} \int_{-\infty}^{\infty} |H(f)|^2 df \qquad (1)$$

where $f_0$ is the frequency at mid-band or the frequency of maximum response. Alternately, [13 Harris, p.54] and [14 Nielsen, p.166] show the equivalent sampled time domain representation, (normalised by $N_0/T$, the noise power per DFT bin), as

$$ENBW = \frac{\sum_n x^2(nT)}{\left(\sum_n x(nT)\right)^2} \tag{2}$$

where $x(nT)$ is the time domain series sampled every $T$ seconds.

Note that the *ENBW* is not the same as the half-power bandwidth (the so called 3 dB bandwidth), although for many receivers this may be a good approximation.

## 2.7 Probability Density Function (*pdf* or *PDF*)

A stationary (ergodic) continuous random signal $x(t)$ takes on an infinite number of values, and the probability of it taking on a particular value is vanishingly small. Thus a useful descriptor for such a signal is the probability that the signal occupies a small range of values. This is essentially an amplitude domain statistic of the signal. Suppose $\delta t/T_0$ is the fraction of time that the signal spends in the range $u$ to $u+\delta u$ over a total time duration $T_0$. Then as $\delta u \to 0$, the probability density function of $x$ at $u$, $pdf_x(u)$ can be defined as

$$pdf_x(u) = \lim_{\delta u \to 0} \left( \frac{\underset{T_0 \to \infty}{Lim} \left( \frac{\delta t}{T_0} \right)}{\delta u} \right). \tag{8}$$

Note also that, by definition,

$$Probability(a \le x \le b) = \int_a^b pdf_x(u)\, du \tag{9}$$

and

$$\int_{-\infty}^{\infty} pdf_x(u)\, du = 1. \tag{10}$$

Examples of some frequently encountered pdfs are given in Appendix A, with a tabulated description of how they relate to detection theory.

## 2.8 Receiver Operating Characteristic (ROC)

A Receiver Operating Characteristic (ROC) is the relationship between Probability of False Alarm ($P_{fa}$), Probability of Detection ($P_d$) and Signal to Noise Ratio (SNR) or alternatively detection index ($d$) as a third parameter. Plots of the resulting functions are known as ROC curves. Appendix B shows how to generate an ROC curve for the Gaussian random variable.

# 3. Detection Threshold Concepts and Theory

## 3.1 Probability Theory and Detection

If there is a continuous signal $s(t)$ and continuous Gaussian noise $n(t)$, respective probability density functions $pdf_s$ and $pdf_n$ can be defined, representing the probabilistic frequency distributions. The signal $s(t)$ can be added to the Gaussian noise $n(t)$ to produce a composite signal $x(t)=s(t)+n(t)$ with resultant probability density function $pdf_x$. Strictly, however, a pdf is only properly defined if the random variable is in some sense stationary [15 Proakis, p.932], (otherwise the pdf may vary with time or some other parameter). Assuming this to be true, then, by definition,

$$Probability(s \le \lambda) = \int_{-\infty}^{\lambda} pdf_s(u)\, du\,, \tag{11}$$

$$Probability(n \le \lambda) = \int_{-\infty}^{\lambda} pdf_n(u)\, du \text{ and} \tag{12}$$

$$Probability(x \le \lambda) = \int_{-\infty}^{\lambda} pdf_x(u)\, du\,. \tag{13}$$

The probability density functions of a signal with noise, $pdf_x$, and noise only, $pdf_n$ may be drawn in the manner shown by the illustrative example of Appendix B as $\phi_{s+n}$ and $\phi_n$ respectively. In this example, the mean of the signal with noise distribution has clearly increased over that of the noise alone. By definition, the total area under a pdf curve must equal unity. What is evident from this graph is that at any selected threshold $\lambda$, the probability of detecting a signal, if a signal is present, is the area under the $\phi_{s+n}$ curve from $\lambda$ to $\infty$, corresponding to the probability of the input exceeding $\lambda$. However, the probability that noise alone could cause the input to exceed the threshold value is in turn given by the area under the $\phi_n$ curve from $\lambda$ to $\infty$. Thus a simple binary detection criterion has been established: for the noise and signal with noise pdf's prevailing, set a $\lambda$ such that when it is exceeded a detection is called, while accepting that this will entail an inevitable probability of false alarm. A decision matrix

can be drawn to illustrate each of the binary possibilities, as in Table 1 below [5 Helmstrom, p.61].

*Table 1. Detection Decision Matrix.*

| | Detection called | No detection |
|---|---|---|
| Signal present | Correct Detection | False Dismissal[1] |
| Signal absent | False Alarm[2] | Correct Dismissal |

[1] Error of the second kind
[2] Error of the first kind

It is evident that there are two independent variables operating. By sensible convention, the primary detection measures of interest are

(a) Probability of correct detection ($P_d$)
and
(b) Probability of false alarm ($P_{fa}$).

Clearly it is also true that:

Probability of false alarm = 1- Probability of correct dismissal, and
Probability of correct detection = 1 - Probability of false dismissal.

Now define a hypothesis, $H_1$, which will be true if there is a signal present with the noise. Further, define $H_0$ to mean the hypothesis that there is no signal present (i.e. there is only noise). Then the probability that a correct detection is made is the conditional probability that, given a signal is present, the input threshold is exceeded:

Probability of correct detection = $P(x(t) > \lambda \mid H_1)$ (14)
or

$$P_d = \int_{\lambda}^{\infty} pdf_{x|H_1}(u)du. \tag{15}$$

Similarly, the probability of a false alarm is the conditional probability that, given there is no signal present, the threshold is exceeded:

Probability of false alarm = $P(x(t) > \lambda \mid H_0)$ (16)
or

$$P_{fa} = \int_{\lambda}^{\infty} pdf_{x|H_0}(u)du. \tag{17}$$

It is next necessary to determine the optimum $\lambda$ to achieve the desired $P_{fa}$ and $P_d$. As $\lambda$ is the threshold SNR required for detection, a minimum value is sought. For example, if $\lambda$ is a function of the phase of the signal, then an average over a $2\pi$ range may be required if the phase can be assumed to be a random variable. Several decision theory approaches to formulating the required (sometimes multidimensional) hypothesis testing equations are addressed in the literature: [7 Whalen, p128], [5 Helmsrom, p.129], [20 Burdic, p364] and [14 Nielsen, p.117], including the use of Maximum Likelihood, Neyman Pearson and Bayes Criterion.

The Bayes Criterion is a method of minimising average risk over the decision space, and can be applied only if all the prior probabilities and their costs are well defined.

It has been shown [14 Nielsen, p101], [14 Nielsen, p.116], [5 Helmstrom, p.130] and [7 Whalen, p.130] that the maximum probability of detecting a signal from a single detection sample, while controlling the incidence of false alarms, given that the a priori probabilities $Pr(H_0)$ and $Pr(H_1)$ are unknown, can be identified by using a Neyman-Pearson detector. This is done by forming a pdf likelihood ratio test $\lambda(u)$, formed such that $H_1$ is chosen if $\lambda$ exceeds $\lambda(u)$, formed as

$$\lambda(u) = \frac{pdf_{H_1}(u)}{pdf_{H_0}(u)} \tag{18}$$

where $u$ is a single observation of the received sequence.

[7 Whalen, Ch7] develops the Neyman-Pearson detector for continuous waveforms whereas [14 Nielsen, p.117] does so for a sampled waveform, so the latter is more useful for analysing digitally based signal processing systems. [12 Meyer and Mayer, p.69] also suggest a trial and error approach based upon the Gram-Charlier series has been found to be useful.

## 3.2 The Sinusoidal Signal in Gaussian Noise

A sampled time domain sinusoidal signal $s(n)$ can be defined by

$$s(n) = A\sin\left(2\pi\frac{f_0 n}{f_s} + \theta\right) \qquad \text{for } n = 0\ldots \text{M-1} \tag{19}$$

where

M = the total number of samples and
$f_s$ = the sampling rate in samples per second.

and then, for a time domain noise function $g(n)$, the received signal $x(n)$ obtained when a sinusoid is present in the noise becomes

$$x(n) = s(n) + g(n)\,. \tag{20}$$

At the receiver, a decision between the two hypotheses, $H_1$:signal present, and $H_0$:signal absent, based on N measurements, then needs to be made, viz.

$$H_1: x(n) = A\sin\left(2\pi\frac{f_0 n}{f_s} + \theta\right) + g(n) \qquad \text{for } n = 0, .., N\text{-}1 \tag{21}$$

or

$$H_0: x(n) = g(n) \qquad \text{for } n = 0, .., N\text{-}1. \tag{22}$$

If $g(n)$ is zero mean white Gaussian noise, then after it has been through a square law (or magnitude squared) device, it has a pdf which can be written: [20 Burdic, p.256]

$$pdf_{|g|^2}(u) = \frac{1}{\sigma_g\sqrt{2\pi u}}\exp\left(-\frac{u}{2\sigma_g^2}\right), \qquad \text{for } u > 0 \tag{23}$$

(A time domain representation is somewhat more complex and is not essential for this discussion). It has been shown [7 Whalen, p.102], [14 Nielsen, p.115], [20 Burdic, p.260] and [21 Tsui, p268] that the pdf of the magnitude (or envelope) function of a narrowband Gaussian process, $g(n)$, is the Rayleigh function,

$$pdf_{|g|}(g) = \frac{g}{\sigma_g^2}\exp\left(-\frac{g^2}{2\sigma_g^2}\right), \qquad \text{for } g > 0 \tag{24}$$

and that the distribution of the envelope of the sinusoidal signal when combined with narrowband Gaussian noise, $pdf_{|x||H_1}$, is the Rician function [7 Whalen, p.105], [21 Tsui, p.270] and [14 Nielsen, p.115],

$$pdf_{|x||H_1}(x) = \frac{x}{\sigma_g^2}\exp\left(-\frac{x^2 + A^2}{2\sigma_g^2}\right)I_0\left(\frac{Ax}{\sigma_g^2}\right), \text{ for } x > 0, \tag{25}$$

where $I_0$ is the modified Bessel function of zero order, defined by:

$$I_0(v) = \sum_{k=0}^{\infty}\frac{v^{2k}}{2^{2n}(k!)^2}\,.$$

Application of the relevant pdfs, using the approach of section 3.1, lead to the results for $P_d$ and $P_{fa}$ outlined in the following paragraphs.

If the receiver threshold level is set at λ, and a detection decision is made from one square law detection measurement, with the phase of the sinusoidal signal randomly distributed between 0 and 2π, then [7 Whalen, p108], [14 Nielsen, p.120] and [21 Tsui, p.274],

$$P_{fa} = \int_{\lambda}^{\infty} \frac{u}{\sigma^2} exp\left(-\frac{u^2}{2\sigma^2}\right) du = exp\left(-\frac{\lambda^2}{2\sigma^2}\right), \tag{26}$$

which can be seen to result from setting A=0 in the expression for $pdf_{|x||H_1}$ above.

If the receiver threshold level is set at λ, and if a detection decision is made from the sum of N square law detected measurements, with the phase of the sinusoidal signal in each measurement randomly distributed between 0 and 2π, then [7 Whalen, p112], [14 Nielsen, p.120] and [21 Tsui, p.275],

$$P_d = \int_{\lambda}^{\infty} \frac{u}{\sigma^2} \exp\left(-\frac{u^2 + \left(\frac{AN}{2}\right)^2}{2\sigma^2}\right) I_0\left(\frac{uAN}{2\sigma^2}\right) du \tag{27}$$

The above expression can be written in the form [12 Meyer and Mayer, Sect 3.4], [14 Nielsen, p.121] and [20 Burdic, p.370],

$$P_d = \int_{\beta}^{\infty} v exp\left(-\frac{v^2 + \alpha^2}{2}\right) I_0(v\alpha) dx = Q(\alpha, \beta) \tag{28}$$

where $Q(\alpha, \beta)$ is the Marcum Q-function [8 Marcum] and [7 Whalen, p.106], which is one minus the cumulative Rician pdf.

An alternative formulation by [22 Williams and Ricker] yields a similar result as follows. If a set of $M$ samples of a signal in white Gaussian noise are to be detected, and a normalised averaged power sample Z produced, then a Fourier transform of duration T (with incoherent integration of the individual transformed samples) results in a $P_{fa}$ defined by the integral of a Chi-square density function as follows:

$$P_{\text{fa}} = \int_{\lambda}^{\infty} 2^{-M} \left(\frac{M}{N}\right)^M \frac{Z^{M-1}}{(M-1)!} \exp\left(-\frac{M}{N} Z\right) dZ \tag{29}$$

and $P_d$ is determined by the integral of a non-central Chi-square density function,

$$P_d = \int_{\lambda}^{\infty} \frac{M}{N^{\frac{M+1}{2}} \left(\frac{S}{N}\right)^{\frac{M-1}{2}}} Z^{\frac{M-1}{2}} \exp\left(-\left\{\frac{MZ}{N} + \frac{MS}{N}\right\}\right) I_{M-1}\left(\frac{2M\sqrt{SZ}}{N}\right) dZ, \qquad (30)$$

where S is the signal power and N the noise power in each sample at the integrator input, $I_{M-1}$ is a Bessel function of order M-1 and $\lambda$ is the detection threshold.

## 3.3 Detection Threshold

The Detection Threshold *DT*, in decibels, for detecting a signal in noise is defined by the signal to noise ratio (*SNR*), as per the following equation:

$$DT = 10Log_{10}\frac{S}{N} = 10Log_{10}(SNR), \qquad (31)$$

where *S* is the signal power in the receiver bandwidth at the input and *N* is the noise power density in the receiver bandwidth at the input to the receiver, required to achieve a specified $P_d$ and $P_{fa}$, which in this report have been chosen to be $P_d = 0.5$ and $P_{fa} = 10^{-4}$. To be of use, it is usually necessary to work with more practical quantities than *S*, *N* and *SNR*, such as the signal plus noise power, as discussed in the next section.

For most narrowband DT studies the input *SNR* is calculated as

$$SNR = \frac{\text{sinusoidal signal power in bandwidth B}}{\text{noise power in 1 Hertz band}}, \qquad (32)$$

noting that the receiver bandwidth B is of course much greater than that of the narrowband signal.

To obtain the detection threshold for a sinusoidal signal in Gaussian noise, a solution minimising $\lambda$ in the $P_d$ and $P_{fa}$ equations in the previous sections needs to be obtained. This is a very difficult mathematical problem [6 Marcum], [9 Robertson ] and [10 Nuttall], but approximate solutions have been obtained, essentially using the decision theory of the Neyman-Pearson criterion, discussed in section 3.1.

## 3.4 Detection Index

If the receiver has a bandwidth B and the noise is white and Gaussian over the receiver bandwidth, then $N=BN_0$, where $N_0$ is the noise power spectral density in a 1 Hz band. Further, as the signal power is rarely a measurable quantity in a detection problem

(that is, it is usually an unknown quantity in a real system), a more useful but related 'SNR' is defined in [1 Lawson and Uhlenbeck], [12 Meyer and Mayer, p.73], [23 Urick, p.382] and [20 Burdic, p.366]: the detection index, $d$, sometimes known as the deflection or detection criterion, where

$$d = \frac{(Mean_{S+N} - Mean_N)^2}{\sigma^2} \tag{33}$$

where

$Mean_{S+N}$ = mean value of the signal in noise at the thresholder
$Mean_N$ = mean value of the noise only at the thresholder
$\sigma$ = standard deviation of noise at the thresholder (assuming $\sigma=\sigma_n=\sigma_{s+n}$)

[4 Peterson *et al.*] have found that for a completely unknown signal in Gaussian noise, if Signal power/Noise power in a 1 Hz band is small and the product of the receiver bandwidth B and signal duration time $T$ is large, then [23 Urick, p.384]

$$d = BT\left(\frac{S}{N}\right)^2, \tag{34}$$

so that DT can then be expressed as

$$DT = 10Log_{10}\sqrt{BT\left(\frac{S}{N_0}\right)^2 \frac{1}{B^2}} \tag{35}$$

where $N$ is the total noise power in bandwidth $B$ and $N_0$ the noise power in a 1Hz band. Hence

$$DT = 5Log_{10}\left(\frac{Bd}{T}\right) \tag{36}$$

If either $S/N$ is large or the bandwidth time product is small then a correction to the above equation is required, as the mathematics reverts to the Equations (29) and (30) above. This occurs in a progressive manner, such that Equation (36) is a satisfactory first approximation.

## 3.5 Receiver Operating Characteristic Curves

Receiver Operating Characteristic (ROC) curves [23 Urick p.381], [12 Meyer and Mayer], (where they are referred to as Meyer plots) and [7 Whalen p.202] are a set of plots of the Probability of False Alarm ($P_{fa}$), versus Probability of Detection ($P_d$), with Signal to Noise Ratio ($SNR$) or detection index ($d$) as a third parameter. The curves result from the probability density functions of the noise alone and signal with noise, measured at the thresholder where detection decisions are to be made. Appendix B

shows an example of a ROC curve applied to detection of a constant signal in Gaussian noise.

ROC curves for a sinusoidal signal in Gaussian noise are obtained by solving for the optimum (in this case minimum) $\lambda$ (or *SNR*) in section 3.1 above, given the noise and signal plus noise pdfs. A closed form solution has only been obtainable for the case of noise alone, with a single sample used for detection. All other cases must be solved using numerical techniques and simplifying approximations.

ROC curves allow *DT* or *MDS* values to be calculated at values of $P_d$ and $P_{fa}$ other than the normalised values. This is necessary, for example, if an experimental measurement of *MDS* is performed, as it is very unlikely that the experimental results from different observers would correspond to $P_d$=0.5 and $P_{fa}$=$10^{-4}$. The ROC curves enable adjustment of the measured *SNR* to the normalised *SNR*, or *MDS*.

# 4. Detecting Sinusoids in Spectrograms

## 4.1 Practical spectral analysis

Spectral analysis is performed to generate an estimate of the power spectrum of the input function. It is this estimate which is used in the detection process described above. The results are usually displayed graphically in some kind of spectrogram or lofargram. Narrowband (sinusoidal) signals are then evident as sharp peaks, or lines, in an otherwise uniform background, because they cause a relatively high local *psd* about their centre frequency.

To maximise the detection index *d*, which is a measure of the systems *SNR*, it has been shown [24 Gardner, p.104] that the periodogram provides optimum detection statistics, for the case of a sine wave in white (band-limited) Gaussian noise with unknown amplitude, phase and frequency.

To obtain accurate predictions of the performance of a spectrogram for the detection of sinusoids in Gaussian noise, some of the practical limitations of realisable measurement techniques and equipment need to be taken into account.

Usually the input time waveform being analysed is continuous and memory and digital signal processor architecture constraints mandate sampling, quantising and blocking of the input waveform. Also, to provide a progressive indication of the results of computations on an ongoing basis requires blocking of the data stream, followed by optional averaging of blocks, to achieve a low pass filtered result. There is a tradeoff here in the smoothness (or smaller variance) in the *psd* estimate versus the frequency resolution [18 Marple, p.132], although for signal detectability the latter would be more important [18 Marple, p.19]. Sometimes exponential averaging is used to provide a weighted filter, where the latest blocks have a greater influence on the output. Recall

also, from Section 2.6 that the power spectral density estimate variance does not approach zero as block size is increased [15 Proakisp.873] - Bartlett's smoothing procedure or some other method must be used to achieve this result [19 Leon-Garcia, p.419].

### 4.1.1 Discrete Fourier Transform (DFT)

The discrete Fourier transform (DFT) and its derivative, the fast Fourier transform (FFT) are the finite time duration (or finite block size) sampled implementations of the Fourier series. The Fourier transform can be defined [15 Proakis, p.175] and [20 Burdic, p.195] as

$$X(f) = \int_{-\infty}^{\infty} x(t) e^{-2\pi i f t} dt \tag{37}$$

where the $X(f)$ are known as the Fourier coefficients of x(t), because

$$x(t) = \sum_{n} X(f) e^{2\pi i f t} \tag{38}$$

(Note that the sign of the power exponent is sometimes inverted in definitions, but this does not affect self consistent derived results, as in for example [16 Press, p.503]). The DFT can then be defined to be the repeating series of length N,

$$X_n = \sum_{k=0}^{N-1} x_k e^{-2\pi i k n / N} \tag{39}$$

where

$x_k$=k$^{th}$ sample of the input waveform, taken at time $t_n = \frac{k}{T}$

$N$=total number of time domain samples (block size)
$T$=DFT input time series length=block size in seconds,
$f_s$=sampling frequency =$N/T$

It is evident that the DFT, unlike the Fourier transform, has finite frequency domain resolution. The FFT is an efficiently computed DFT, and therefore yields the same $X_n$ values.

The ability to be able to process the sampled input data only in fixed, finite sized blocks results in a well defined frequency resolution equal to $f_r$, where

$$f_r = \frac{1}{T} = \frac{f_s}{N}. \tag{40}$$

This resolution, in turn, defines how finely the psd function of the input waveform is being analysed. Further, each discrete frequency bin from the DFT can be viewed as

essentially the output of a narrrowband filtering operation [25 Altes] and [14 Nielsen, p.158].

One improvement upon the simple DFT process can be achieved by overlapping the blocked data processing, thereby introducing redundant processing. The penalty is clearly an increased computational demand. However, the partitioning of the input data samples into blocks without maintaining phase continuity irrevocably removes block to block coherence. This is discussed in Section 5.2. If the signal to be detected is a continuous sinusoid, this loss of coherence introduces a theoretical detection performance loss [14 Nielsen, p.122] and [7 Whalen, p.205]. Other than DFT techniques are required to avoid this detection threshold penalty, such as form correlation, matched field processing [24 Gardner, p.107] or parametric techniques [14 Marple, p.172].

### 4.1.2 Windowing

It is often necessary to not only detect a narrowband signal in noise, but simultaneously resolve closely spaced signals. Also, in many applications, the spectrum is cluttered with signals, many of which are of minimal interest to the observer. This results in desired signals being smeared, obscured or swamped, through a process of spectral leakage [13 Harris] and [15 Proakis, p.861]. Application of a well chosen time domain weighting function, or window function, to the blocked, time sampled data prior to a DFT operation, dramatically improves the adjacent tonal discrimination [13 Harris ], [26 Nuttall], [27 Hamming], [28 Blomqvist], [29 Gade] and [30 Geckinli]. The process is known as windowing. However, the penalty in achieving this superior discrimination is increased equivalent noise bandwidth, corresponding to an increased main lobe width, which translates directly into a DT penalty (i.e., an increase in DT). This is the result of the wider main lobe allowing more noise power through to the detector, even though sidelobe levels are reduced.

Figure 3 illustrates the effect of windowing on a simple sinusoid. First, (a) the sinusoidal frequency is chosen to be exactly central to a DFT bin. The magnitude of the DFT result (b) then shows as a pure tonal. Next (c) shows the effect of the sinusoid not being bin central, producing high levels of undesirable spectral leakage (d). Finally, (e) is the result obtained when the non-central sinusoid is Hann windowed and then (g) is the corresponding DFT. Although a wider main lobe is evident, broad spectral leakage is clearly more controlled. Real time processors often need to further compromise in their choice of windowing function, to reduce the computational load. As a result, the 'Von Hann' or simply 'Hann' or 'Hanning' window, which is the raised cosine function with initial and final values of zero, is widely used.

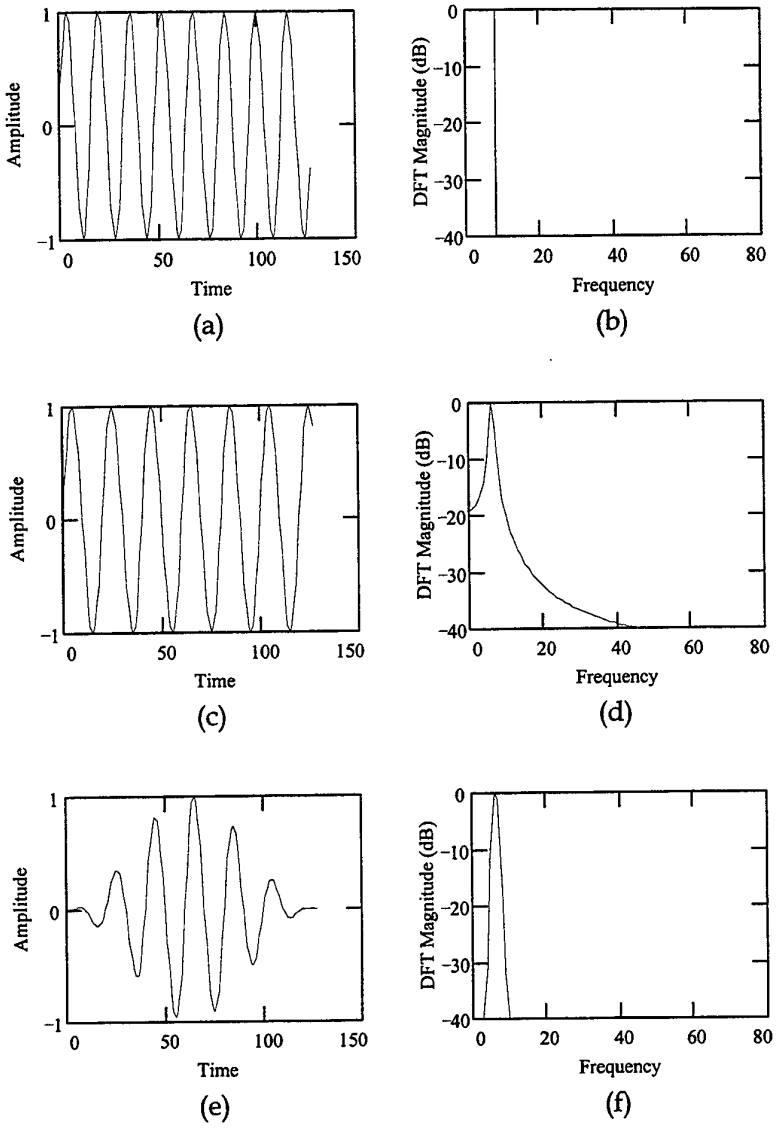


*Figure 3. Windowing of a sinusoidal waveform.*

### 4.1.3 Scalloping

Scalloping is an effect of windowing, causing the main lobe of the frequency response of the window function to be maximum only at the centre of a frequency bin, and reducing to a minimum at the frequency corresponding to the mid-point between adjacent pixel bins [30 Hamming, p.116] and [39 Bendat, p.394]. Thus the individual DFT frequency bin responses, when combined, result in an overall fluctuating system response as a function of frequency. A sinusoid which happens to be exactly between

two adjacent bins then suffers a maximum scalloping attenuation, or loss. A randomly placed sinusoid would, on average, suffer the average scalloping loss. Therefore the average loss is often particularly significant for experiments employing sinusoids of random frequency, and real world signals. The average scalloping loss is defined by [14 Nielsen, p38] and [31 Pryor, p.27] as,

$$SL_{av}(dB) = 10Log_{10}\frac{|W(0)|^2}{\frac{N}{f_s}\int_{\frac{f_s}{2N}}^{\frac{f_s}{2N}}|W(f)|^2\,df} \tag{41}$$

where

$W(f)$ = Fourier transform of the windowing function at frequency f,
$N$ = DFT block size and
$f_s$ = input data sampling rate used by the DFT.

The rectangular window has maximum scalloping loss [14 Nielsen, p38 and p171]. Scalloping loss versus DFT bin spacing for various filter types is plotted in [31 Pryor, p28] and maximum losses have been tabulated by [13 Harris]. Examples of the magnitude of the scalloping effect are given in Table 2 below.

*Table 2. Scalloping Loss (dB) for Narrowband Detection*

| Window type | Minimum Loss | Maximum Loss | Average Loss |
|---|---|---|---|
| Rectangular | 0 | 3.92 | 1.25 |
| Hann | 0 | 1.42 | 0.5 |

## 4.2 Summary of published solutions

### 4.2.1 Urick and Nuttall Power Law Detector Model

For power law detection of a sinusoidal signal in Gaussian noise, modelled as shown in Figure 4, [23 Urick] uses the work of [32 Nuttall] and [4 Petersen *et al.*], to develop a model for DT as,

$$DT = 5Log_{10}\left(\frac{Bd}{T}\right) + Correction_{finiteBT} \tag{42}$$

where
$B$ = narrowband filter bandwidth,
$d$ = detection index,
$T$ = total integration time and
$Correction_{finiteBT}$ = finite bandwidth-time correction term

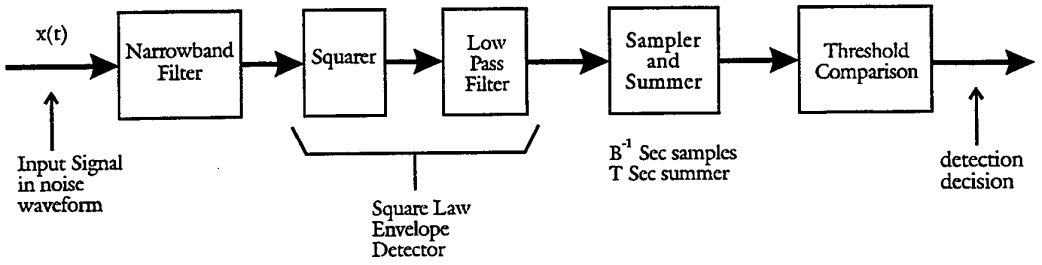


*Figure 4. Nuttall (Ref. 32) power law detection model*

The first term in the above equation applies to a single detection sample of a Gaussian statistic, and the second term, under the standard conditions of $P_d = 0.5$ and $P_{fa} = 10^{-4}$, is empirically approximated by $Correction_{finiteBT} \approx 3.79(BT+1)^{-0.406}$ dB [26 Nuttall], and compensates for the deviation from Gaussianity at small bandwidth time products. [20 Burdic, p.380] shows a similar correction relationship. Appendix C explains the origins of this approximation and method used to compute it.

### 4.2.2 Nielsen Linear Envelope Detector Model

The sampled amplitude (or linear) detector has been numerically evaluated by [9 Robertson] for a sinusoidal signal in narrow band Gaussian noise. Receiver Operating Characteristic (ROC) curves have been produced showing the relationship between output SNR, Probability of Detection and Probability of False Alarm. [9 Robertson] also found that for $P_d$=0.5, if an error, of magnitude always less than 0.2 dB, is acceptable, and the standardised threshold scale changed, the curves can also be applied to the square law detector. Use of the linear vs. quadratic detector comparison curve [9 Robertson], [12 Meyer and Mayer, p.69], [7 Whalen, p.263] and [14 Nielsen, p.169] could allow this approximation error to be corrected for. When relatively large $P_{fa}$ values apply (between $5.0\times10^{-4}$ to $9.0\times10^{-2}$) with $P_d$=0.5, the difference between linear and square law detectors progressively diminishes to [-0.1, +0.2] dB [9 Robertson]. For M=1, however, linear and power law detectors have the same performance. In general, an error of 0.2 dB theoretically corresponds to a maximum error of a few percent in the probability of detection [12 Meyer and Mayer, p.64].

More recently, [11 Albersheim] has empirically determined an accurate (to within 0.2 dB) closed form expression for the [9 Robertson] solutions, yielding the ROC curve detection index (or output *S/N*) given a required Probability of Detection, Probability of False Alarm and number of independent samples, for the linear envelope detector. The [11 Albersheim] expression has been tested over $P_{fa}$= $10^{-3}$ to $10^{-7}$, $P_d$=0.1 to 0.9 and M=1 to $2^{13}$ (8096). The expression is

$$S/N \text{ (dB)} = -5\log_{10}M + \left(6.2 + \frac{4.54}{\sqrt{M+0.44}}\right)\log_{10}(A + 0.12AB + 1.7B), \quad (43)$$

where

$$A = \ln\frac{0.62}{P_{fa}}$$

$$B = \ln\frac{P_d}{1-P_d} = \ln(P_d) - \ln(1-P_d)$$

Setting $M = K_I$ and recognising that the $SNR$ at the output, $S/N = dK_I$ [14 Nielsen, p.167], the theoretical $DT$ estimate can then be expressed as,

$$DT = 10Log_{10}\left(\frac{f_s}{N}\right) + 10Log_{10}ENBW + SL + PL - 5Log_{10}(K_I) + 5Log_{10}(d) \quad (44)$$

where

$\frac{f_s}{N}$ = sampling rate / number of samples per DFT = DFT frequency bin resolution,
$ENBW$ = equivalent noise bandwidth of the pre-DFT windowing function,
$SL$ = average scalloping loss of the DFT window used,
$PL$ = practical processor implementation loss. Set to zero for an ideal processor,
$K_I$ = effective number of independent samples,
= (DFT filter bandwidth) (observation time), and

$5\log_{10}d = \left(6.2 + \frac{4.54}{\sqrt{K_I+0.44}}\right)\log_{10}(A + 0.12AB + 1.7B)$, with $A$ and $B$ as above.

(Note: The graph of this function in [14 Nielsen, p.169] does not appear to be plotted accurately. It is best to use the above equation)

### 4.2.3 Pryor Power Spectrum Detector Model

For a DFT power spectrum analyser, the [31 Pryor] expression developed for estimating the DT of a sinusoid in Gaussian noise is

$$DT = Sensitivity_{basic} + \Delta MDS_{FAP} + \Delta MDS_{Pd} + \Delta MDS_{Td} + \Delta MDS_{NBW,Fn} + \Delta MDS_{scalloping} + \Delta MDS_{ALIsampling} \quad (45)$$

where

$Sensitivity_{basic}$ = $5\log_{10}(B) - 5\log_{10}(T)$, with post detection integration (i.e., $T >> 1/B$)
= $S/N$ (dB) for $P_d$=50% and $P_{fa}$=16%

$\Delta MDS_{FAP}$ = correction to desired false alarm rate, $\sim 3.607(BT)^{-0.35} + 5.511$ from [31 Pryor, Fig 4], ~+6.7 dB for $P_{fa}$= $10^{-4}$,

$\Delta MDS_{Pd}$ = correction if a $P_d$ other than $P_d$=0.5 is required,

$\Delta MDS_{Td}$ = correction for effect of exponential integration with a finite observation time, (if applicable, see [31 Pryor Figure 7]),

$\Delta MDS_{NBW,Fn}$ = correction for practical bandpass filter function implementation on the noise spectrum, (+0.17 dB for a Hann weighted correlator, [31 Pryor, Table 1]

$\Delta MDS_{scalloping}$ = correction for response of bandpass filter on signal, (+1.4 dB maximum, +0.5 dB average for Hann filter, [31 Pryor, Figure 9] and

$\Delta MDS_{ALIsampling}$ = bandpass filter post detection sampling loss, (+1.59 dB for Hann window function [31 Pryor, Figure 11]).

### 4.2.4 Williams and Ricker Sinusoid in Gaussian Noise Model

The general *MDS* equation for sinusoids of unknown frequency, in white Gaussian noise, referenced to noise in a 1Hz band and expressed as the SNR at the input is, from [22 Williams and Ricker],

$$S_{md} = -G_c - G_i(t) - G_r(t) - G_r(f) + L_r + \alpha_{fa} + L_{imp} \qquad (46)$$

where

$S_{md}$ = minimum detectable signal to noise ratio,

$G_c$ = -10Log$_{10}B_N$ , the coherent integration gain,

$B_N$ = filter equivalent noise bandwidth

$$= \frac{1}{2\pi j}\int_{-j\infty}^{j\infty} |W(s)|^2\, ds\,,$$

$W(s)$= Laplace transform of the band limiting filter transfer function,

$G_i(t)$ = the gain from $\tau B_N$ postdetection integrations,
where $\tau$ = duration of the signal. For $P_d$ = 0.5 and $P_{fa}$ = $10^{-4}$,
this gain can be approximated by the function
5Log$_{10}$($\tau B_N$)+4(1-exp[-0.9*log$_{10}$($\tau B_N$ )]), to within ~0.1 dB.

$G_r(t)$ = gain from time redundancy between power samples,

$G_r(f)$ = average frequency redundancy gain,

$L_r$ = average ripple loss between DFT bins, (i.e., average scalloping loss),

$\alpha_{fa}$ = decision threshold in dB for specified detection criteria with $M$=1.
In particular, $\alpha_{fa}$ = +9.4 dB for $P_d$ = 0.5 and $P_{fa}$ = $10^{-4}$ ,
(From [22 Williams and Ricker, Figure 2]) and

$L_{imp}$ = implementation loss, (zero for an ideal processing system).

The above equation may be further summarised as

$$MDS = 10Log_{10}B_r - G_i(t) - \alpha_{fa} + X, \tag{47}$$

with

$B_r$ = resolution bandwidth of the spectral analysis.

*Table 3. Values of X (and $L_r$), in dB units, for two window and overlap parameters.*

| Window type | No DFT overlap | ($L_r$) | High DFT overlap | ($L_r$) |
|---|---|---|---|---|
| Rectangular | 1.1 | (1.1) | 0.2 | (1.1) |
| Hann | 2.7 | (0.9) | 0.2 | (0.9) |

## 4.3 Comparison of published results

To compare the above authors' approaches, Table 4 computes the predicted DT for a sinusoid in Gaussian noise prefiltered by a Hann window, DFT analysed with 1 Hz bin resolution, and with the output integrated over 100 seconds. Non overlapped DFT processing is assumed.

*Table 4. Comparison of Predicted Detection Thresholds (dB).*

| Analyst | Model MDS Prediction | Model - Average |
|---|---|---|
| 1. Urick (Ref. 23 ) | -2.44* | -0.95* |
| 2. Modified Urick (Ref. 23 ) | -1.74 | -0.25 |
| 3. Nielsen (Ref. 14) | -1.51 | -0.02 |
| 4. Pryor (Ref. 31) | -1.48 | 0.01 |
| 5. Williams&Ricker (Ref. 22) | -1.24 | 0.25 |
| **Average of 2,3,4 and 5** | **-1.49** | |

* Using the simpler method of accounting for the *ENBW* of a Hann window.

This comparison shows that a simplistic treatment of ENBW in the [24 Urick] model, where $B$ is replaced by ENBW*$B$, is inadequate (by 0.7 dB), when compared to a more rigorous analysis. Using the more rigorous ENBW analysis then gives a mean of the model predictions as $MDS_{mean}$ = -1.49 dB. The peak variation between the models is only 0.25 dB. This is very good agreement, especially given that numerical solutions published in graphical form needed to be applied - and that curve fit approximations to the graphical solutions have been used in some of this report, which in turn are usually only accurate to 0.1 or 0.2 dB.

The [24 Urick] model has an advantage in being presented as an extension to simple Gaussian behaviour, allowing for easy approximations, usually accurate to within a couple of dB, to be made. However, on the strength of the above agreement, and given

that [14 Nielsen] and [11 Albersheim] have the easiest, closed form, acccurate model implementation, it is suggested that they be the preferred model for DT predictions.

Accuracy of the [14 Nielsen] model is ±0.2 dB from the [11 Albersheim] curve fitting and ±0.2 dB resulting from solution of the linear (envelope) rather than power law detection case. Hence overall, over the range $P_d$=0.1 to $P_d$=0.9 and $P_{fa}$=$10^{-3}$ to $P_{fa}$=$10^{-7}$ and $BT$=1 to $BT$=8196, theoretical prediction accuracy is always within ±0.4 dB, and on average can be expected to be better. For the important and often used case of $P_d$=0.5, use of the term $3.78/\sqrt{M}$ in place of $4.54/\sqrt{M+0.44}$ in the [11 Albersheim] expression, Equation 44 may improve the accuracy at M=1 and M>64. Finally, if one considers curve fitting error and linear versus square law error as independent variables, then the root mean square DT error for $P_d$=0.5, $P_{fa}$>5.0x$10^{-4}$ and M<2048 is $\sqrt{0.15^2+0.2^2}=0.25$ dB.

# 5. Practical Lofargram Display Limitations

## 5.1 Visual Integration Gain (VIG)

When a human observer examines a lofargram to detect sinusodial signals, a visual and mental process of integrating the patterned brightness of columns of pixels occurs. Human vision appears to be oriented toward efficient pattern recognition rather than accurate collinear numerical integration as is implicitly assumed in detection theory. Thus it is not surprising to find that as the number of rows of pixels in a lofargram increases, narrowband detection performance does not always show the full improvement predicted by theory [33 Mohindra and Smith ]and [34 Dawe and Grigorakis]. This drop off in visual integration ability results in a loss, or penalty, when compared with the theoretical integration gain available, although this may not be significant for all display configurations [35 Webster]. Sonar operators frequently use 'eye integration', whereby a lofargram is viewed at a very shallow angle rather than directly facing the display surface, to minimise the visual integration (VIG) penalty and so improve the visibility of weak 'lines', with considerable effect. That is, VIG is dependent upon the subtended arc to the viewed display surface.

Consider the detection threshold for a Gaussian signal in Gaussian noise with detection bandwidth B (which [23 Urick] refers to as w) and integration time $T$, where $BT$>>1 and the signal to noise ratio can be considered small. Then the detection threshold, DT, is [23 Urick, p.385],

$$DT = 5Log_{10}\left(\frac{dB}{T}\right) \tag{48}$$

Now if the total integration time for a lofargram display is composed of *ndl* display rows, each representing $T_0$ seconds of integration,

$$T = ndl.T_0 \tag{49}$$

from which

$$DT = 5Log_{10}\left(\frac{dB}{T_0}\right) - 5Log_{10}(ndl) \tag{50}$$

However, [34 Dawe and Grigorakis], have found that, for one case of simulated lofargrams generated from a Gaussian stochastic process,

$$DT = 5Log_{10}\left(\frac{dB}{T_0}\right) - 5Log_{10}(ndl) + VIG(ndl) \tag{51}$$

where VIG(*ndl*) is a visual integration penalty (VIG ≥ 0), being the difference between the observed and theoretically computed DT's for the particular representative lofargram style display which was used. That is, there was a human factor 'visual integration' loss. For the configuration measured, the VIG penalty was

$$VIG \text{ (dB)} = 1.38\,log_{10}(ndl) + 0.196(ndl)^{0.65} \tag{52}$$

Figure 5 illustrates the VIG obtained from some simulated lofargrams when using trained sonar observers [34 Dawe and Grigorakis]. The error bars are one standard deviation, measured at each *ndl*.

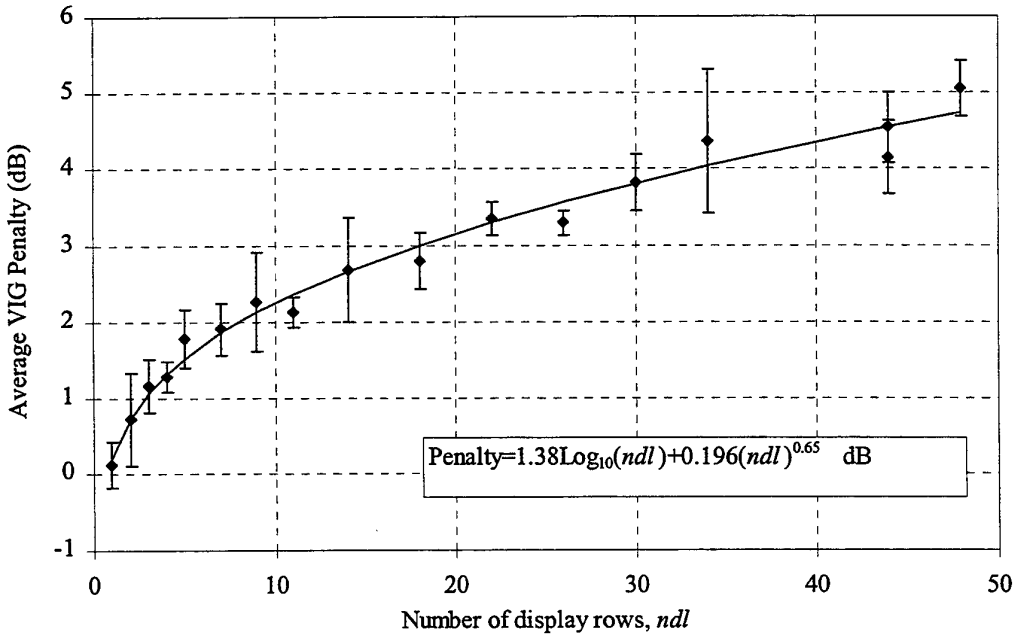


*Figure 5. VIG penalty example from [34 Dawe & Grigorakis].*

## 5.2 Coherent Integration Loss

When analysis of a signal in noise requires an incoming waveform of length $T$ to be blocked into sub-sections of length $T_0$, such that $T = N.T_0$, if phase continuity from block to block is not maintained (such as when a Discrete Fourier Transform is calculated), phase information is lost and a larger minimum detectable signal to noise ratio results [25 Altes]. A larger SNR corresponds to poorer performance. Of course, there is phase coherence within each block, but the process of incoherent block processing cannot be completely undone, even with overlap DFT processing (except for the trivial exception of $N$=1). Examples of the difference in detection performance between coherent and incoherent summation processing can be seen in [7 Whalen, p.205], [31 Pryor], [9 Robertson], [22 Williams and Ricker], [32 Nuttall and Garber] and [12 Meyer and Mayer, p.25]. [22 Williams and Ricker, Figure 6], clearly shows the magnitude of this theoretical difference. An approximation to the amount by which incoherent processing provides lower gain than coherent, i.e., the incoherent integration penalty, $I_p$, for the case of $p_d$=50% and $p_{fa}$=0.01%, is given by Equation 53.

$$I_p \text{ (db)} = 4.9\log_{10}(M) - 4\left(1 - exp(-0.9\log_{10}(M))\right) \qquad (53)$$

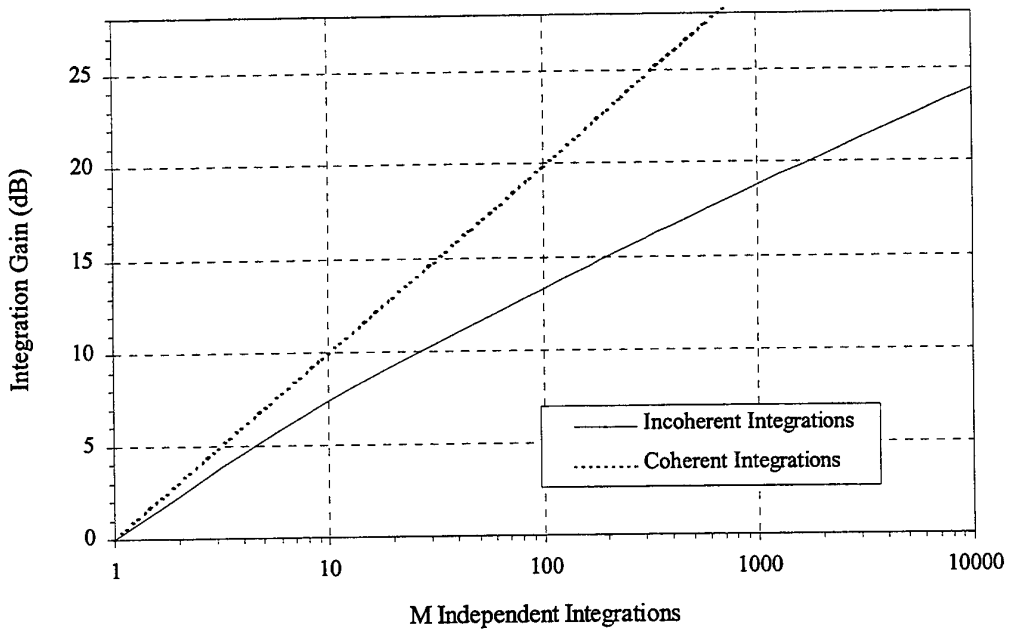


*Figure 6. Coherent and incoherent integration gain.*

## 5.3 Quantisation

When a continuous waveform is to be represented digitally, a virtually random quantisation error is added to the signal, effectively reducing the signal to noise ratio. This quantisation error is due to the finite set of numbers available for digital storage. In other words, an irreversible error signal is added to the input waveform. Binary quantisation is an extreme example of this, where a signal is represented by a zero or one only. In most computations, and certainly those utilising floating point processors, quantisation is an invisible process unless poorly conditioned calculations are undertaken.

At the machine to man interface, however, display technology often has a very limited dynamic range, when compared to the relatively large dynamic range of human vision. This means that the range of easily discriminable brightnesses available from a display screen may be as few as six or eight. In the past , it had been suggested in [36 Marchment] that no more than eight grey levels on a display should be used. This reduction in the ability to resolve the magnitude of a signal by use of intensity modulation may cause a measureable display quantisation loss. [34 Dawe and Grigorakis] have shown an example of the effect of intensity quantisation on a simulated lofargram type display with 8 levels of grey shading: that is, quantisation to 3 bits, and this is reproduced here as Figure 7.

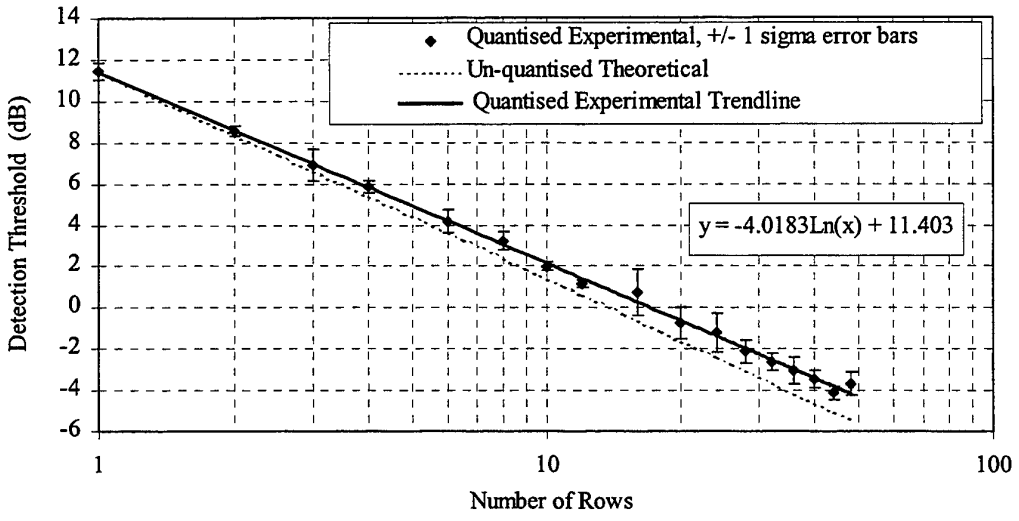


*Figure 7. Quantisation loss of a lofargram display with 8 intensity levels.*

## 5.4 Spectral normalisation

When a lofargram is used to display the power spectral density of a real acoustic signal, rather than white Gaussian noise, the spectrum is often far from uniformly flat.

Usually there are high levels at low frequency, tapering off as frequency rises [23 Urick, p209]. If pixel intensity were assigned such as to cover the entire resulting dynamic range, the low frequency pixels would be saturated with brightness and the high frequency region would be black. Clearly, this would prevent any subtle variations in local signal level, such as a narrowband tonal, from being seen optimally.

One effective solution to this dynamic range problem is spectral normalisation. A local (boxcar) average of adjacent pixel intensities in the same row is used to redefine, or normalise, the local mean for each pixel in turn. This is carried out independently for each display row, and is referred to as boxcar averaging. It has been found that this process has minimal effect upon the visibility of sinusoidal signalss, while dramatically reducing the dynamic range required of the display. An example of the resultant display is shown by Figure 8. Note the stepped effect on the background noise in the vicinity of the three strong signals, due to the boxcar width.

Estimates on the effect on MDS calculated by [40 Parker] are, for a boxcar width of 9 cells, the loss is 0.5 dB and for a boxcar width of 33 cells, the loss is 0.13 dB.

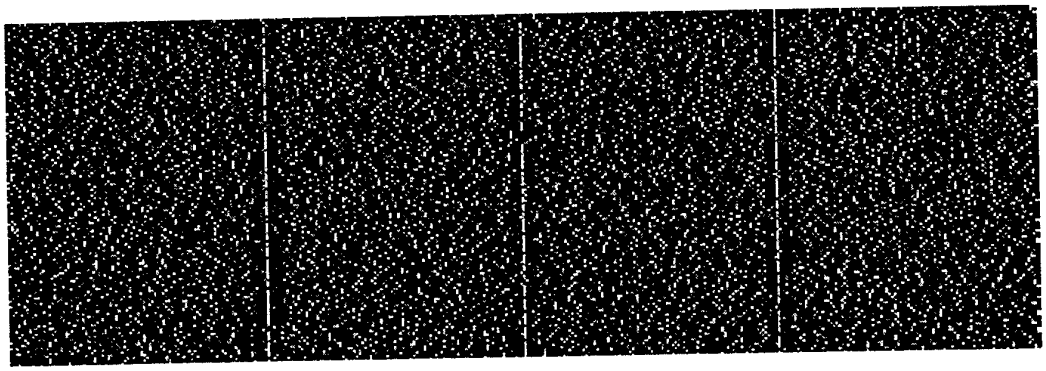

*Figure 8. A lofargram with 9 cell spectral normalisation applied.*

## 5.5 Double Threshold Detection (Binary Detection)

When observing a lofargram display, an operator is actually implementing a double threshold detection process [12 Meyer and Mayer, p.99] and [31 Pryor, p.40]. A thresholder, internal to the processor, allocates grey scale values to pixel elements for display and then the operator later uses visual integration and thresholding to implement a second level of detection decisions. For example, an operator will not have an opportunity to make detections if the relevant pixels have not passed through the first detection stage successfully. This theoretically leads to a combinatorial decision process, possibly modifying the originally determined probabilities for detection and false alarm. This effect is often written off as a "Display Loss".

### 5.6 Multiple Sinusoids per Lofargram

Use of a periodogram to obtain detections via the maximum likelihood estimate of a sinusoid in Gaussian noise, through use of the psd estimate of a waveform, is relatively simple. However this simplicity may not extend to a time series containing more than one sinusoid [24 Gardner, p.340] and [23 Urick, p.390], unless the number of such sinusoids is known and the separation between their frequencies greatly exceeds $1/T$ [37 Walker].

If $m$ statistically independent (orthogonal) signals of the same energy are to be detected, a modified ROC curve applies [23 Urick, p.391], approximated by

$$P_d = 1 - \Phi^{m-1}(\lambda)\Phi(\lambda - \sqrt{d}) \tag{54}$$

and

$$P_{fa} = 1 - \Phi^m(\lambda), \tag{55}$$

where

$$\Phi(\lambda) = \frac{1}{\sqrt{2\pi}} \int_{-\infty}^{\lambda} e^{-\frac{t^2}{2}} dt. \tag{56}$$

To estimate the magnitude of this effect, consider the case of Gaussian statistics, with $P_d$=50% and $P_{fa}$=0.008%: this gives $d$=16. If the signal may be received in either of 10 bins, then m=10 and from the modified ROC curves, [23 Urick, p.391], $P_{fa}$ must be revised to $P_{fa}$=0.05%, corresponding to a Gaussian $d$~11.5. From Equation 48, the change in DT is then approximated by

$$\Delta DT = 5Log_{10}\left(\frac{d}{d'}\right) = 5Log_{10}(1.39) = 0.72dB \tag{57}$$

However, whether a particular experimental setup needs to be analysed according to the requirements for multiple channel orthogonal signal processing must be determined very carefully. [38 Nolte and Jaarsma] develop a model which can be examined for this compliance.

## 6. Conclusion

The convenience and accuracy of the work by [9 Robertson] and [11 Albersheim ], as summarised in [14 Nielsen], is the recommended source for theoretical predictions of omnidirectional narrowband detection performance. Estimated accuracy of the predictions is ±0.4 dB worst case, but usually ±0.2 dB represents the average uncertainty. The validity of the calculations is confirmed by consistency with the work of other analysts, in particular [10 Nuttall].

There are several potential departures from the theoretical DTs calculated by [14 Nielsen], when applied to lofargram displays. The corrections can be significant - for example quantisation and normalisation processes may acount for several tenths of a dB each; however as they are often dependant on human factors or implementation method, each experimental setup would require specific investigation.

# 7. References


1. Lawson, James L. and Uhlenbeck, George E. (1950) *Threshold Signals,* MIT Radiation Laboratory series, **Vol. 24**, Sec. 8.10, McGraw Hill Bolk Company, New York, NY, USA.

2. Harrington, J. V. (October 1950) *Signal to Noise Improvement Through Integration in a Storage Tube,* Proc. I.R.E., **Vol. 38**, p.1165.

3. Reich, Edgar and Swerling, Peter, (March 1953) *The Detection of a Sine Wave in Gaussian Noise,* Journal of Applied Physics, **Volume 24**, Number 3.

4. Peterson, W. W.; Birdsall, T. G. and Fox, W. C. (September 1954) *The Theory of Signal Detectability,* Transactions of the IRE, (1954 Symposium on Information Theory), PGIT-4, p. 171.

5. Helstrom, C. W. (1960) *Statistical Theory of Signal Detection,* Pergamon Press, Oxford Great Britain.

6. Marcum, J. I. (July 1948) *A statistical Theory of Target Detection by Pulsed Radar, Mathematical Appendix,* Rand Corporation Report RM-753.

7. Whalen, A. D. (1971) *Detection of Signals in Noise,* Academic Press, New York USA.

8. Marcum, J. I. (January 1950) *Table of Q-Functions,* Rand Corp. Report RM-339.

9. Robertson, G. H. (April 1967) *Operating Characteristics for a Linear Detector of CW Signals in Narrow-Band Gaussian Noise,* Bell System Technical Journal Volume XLVI, Number 4.

10. Nuttall, A. H. and Magaraci, A. F. (20 October 1972) *Signal-to-Noise Ratios Required for Short-Term Narrowband Detection of Gaussian Processes,* Naval Underwater Systems Centre, Technical Report 4417.

11. Albersheim, W. J. ( July 1981) *A Closed Form Approximation to Robertsons Detection Characteristics,* Proceedings of the IEEE, **Vol 69**, No. 7.

12. Meyer, Daniel P. and Mayer, Herbert A. (1973) *Radar Target Detection,* Academic Press, New York USA.

13. harris, fred J. (January 1978) *On the Use of Windows for Harmonic Analysis with the Discrete Fourier Transform,* Proceedings of the IEEE, **Vol. 66** No. 1.

14. Nielsen, R. O. (1991) *Sonar Signal Processing,* Artech House, Boston USA.

15. Proakis, J. G. and Manolakis, D. G. (1992) *Digital Signal Processing* second edition, Macmillan Publishing Company USA.

16. Press, W. H.; Teukolsky, S. A.; Vetterling, W. T. and Flannery, B. P. (1994) *Numerical Recipes in C,* second edition, Cambridge University Press, Cambridge USA.

17. Hodgekiss, W. S. and Anderson, V. C. (January 1980) *Detection of Sinusoids in Ocean Acoustic Background Noise,* J. Acous. Soc. Am. 76(1).

18. Marple, S. L. Jr. (1987) *Digital Spectral Analysis with Applications,* Prentice Hall Inc. New Jersey USA.

19. Leon-Garcia, Alberto (1989) *Probability and Random Processes for Electrical Engineering,* Addison-Wesley Publishing Company, Massachusetts, USA.

20. Burdic, William S. (1991) *Underwater Acoustic System Analysis,* second edition, Prentice-Hall, New Jersey USA.

21. Tsui, James (1995) *Digital Techniques For Wideband Receivers,* Artech House, Norwood USA.

22. Williams, Jack R. and Ricker, George G. (September 1978) *Spectrum Analyser Overlap Requirements and Detectability using Discrete Fourier Transform and Composite Digital Filters,* The Journal of the Acoustic Society of America, **Vol. 64,** No. 3.

23. Urick, R. J. (1983) *Principles of Underwater Sound,* third edition, McGraw Hill, New York USA.

24. Gardner, W. A. (1988) *Statistical Spectral Analysis,* Prentice Hall, New Jersey, USA.

25. Altes, Richard A. (April 1980) *Detection, estimation and classification with spectrograms,* Journal of the Acoustical Society of America, 67(4), p. .

26. Nuttall, Albert H. (February 1981) *Some Windows with Very Good Sidelobe Behaviour,* IEEE Transactions on Acoustics, Speech and Signal Processing, **Volume ASSP-29,** Number 1.

27. Hamming, R. W. (1989) *Digital Filters* third edition, Prentice Hall Inc. New Jersey USA.

28. Blomqvist, Ake (March 1979) *Figures of Merit of Windows for Power Density Spectrum Estimation with the DFT*, Proceedings of the IEEE, **Vol 67**, No. 3, p. 438.

29. Gade, Svend and Herlufsen, Henrik (March 1988) *Windows to FFTAnalysis*, Sound and Vibration, Instrumentation Reference Issue, p.14.

30. Geckinli, Nezih C. and Yavuz, Davras (December 1978) *Some Novel Windows and a Concise Tutorial Comparison of Window Families*, IEEE Transactions on Acoustics, Speech and Signal Processing, Volume **ASSP-26**, Number 6.

31. Pryor, C. N. (2 August 1971) *Calculation of the Minimum Detectable Signal for Practical Spectrum Analysers*, Naval Ordnance Laboratory, NOLTR 71-92.

32. Nuttall, A. H. and Garber, R. (28 September 1971) *Receiver Operating Characteristics for Phase-Incoherent Detection of Multiple Observations*, NUSC Technical Memorandum No. TC-179-71.

33. Mohindra, N. K. and Smith, M. J. (December 1985) *Visual Detection Thresholds for Simulated Sonar Signals: the Effects of Signal Characteristics, Presentation Mode, Clutter and Reduced Time History*, Technical Memorandum AMTE(S) TM85402 Admiralty Research Establishment (Marine Technology) U. K.

34. Dawe, R. L. and Grigorakis, A. (1996) *A Study of the Visual Integration Gain Component of Detection Threshold for LOFAR Displays*, Research Report, Defence Science and Technology Organisation, Australia (DRAFT).

35. Webster, Roger J. (April 1993) *Minimum Detectable Signal for Spectrogram Displays*, IEEE Transactions on Signal Processing, **Volume 41**, Number 4.

36. Marchment, J. (5-7 July 1994) *LFA Sonar Display Considerations*, UDT Conference Proceedings, Wembly Conference Centre, London U.K. Nexus Business Communications Limited.

37. Walker, A.M. (1971) *On the Esimation of a Harmonic Component in a Time Series with Independent Residuals*, Biometrica 58:21-36.

38. Nolte, L. W. and Jaarsma, D. (1967) *More on the Detection of One of M Orthogonal Signals*, J.Acoust. Soc. Am, 41:497.

39. Bendat, J. S. and Piersol, A. G. (1986) *Random Data Measurement and Analysis Procedures*, second edition, John Wiley and Sons Inc. New York USA.

40. Parker, E. J. (May 1995) *Personal Correspondance,* Maritime Operations Division, Defence Science and Technology Organisation, Salisbury, South Australia.

41. Randall, R. B. (September 1987) *Frequency Analysis* 3rd. edition, 1st. print, Bruel&Kjaer, Printed in Denmark.

# Appendix A:
# Frequently Occurring PDFs in Detection Theory

If.a signal is combined with narrowband Gaussian noise and subjected to an envelope or power law function, the distribution function of the result is as shown in Table A.1. This is then the input to the next stage of the detection process, the thresholder.

*Table A.1 Probability density functions at the output prior to detection*

| Detection process | Input signal type (in Gaussian noise) | Output probability density function | |
|---|---|---|---|
| | | For a Single sample | For Many samples |
| Amplitude | sinusoid | Rician (generalised Rayleigh) | approaches Gaussian |
| Amplitude | Gaussian | Rayleigh | approaches Gaussian |
| Power | sinusoid | Chi-squared, order n* | approaches Gaussian |
| Power | Gaussian | Chi-squared, order n | approaches Gaussian |

* For small sinusoidal signal to Gaussian noise power ratios

If the input to a quadratic detector is a narrowband Gaussian process, the output will be chi-squared distributed [1 Whalen, Section 4.6].

Some interesting or important probability density functions which arise are:

1. The pdf of a sinusoid from [2 Bendat and Piersol, p.53] is:

$$p(x) = \frac{1}{\pi\sqrt{X^2 - x^2}} \qquad \text{for } |x| < X,\ p(x) = 0 \text{ otherwise} \qquad \text{(A.1)}$$

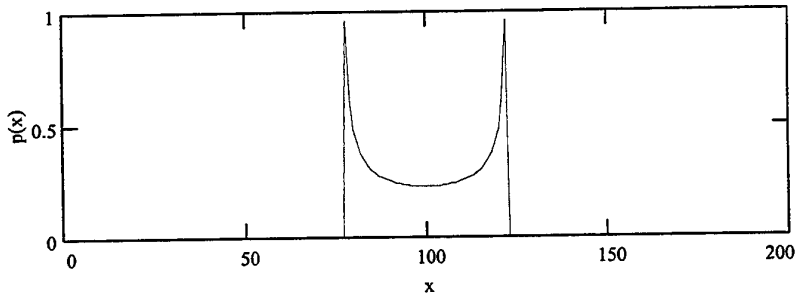


*Figure A.1 An example of a sinusoidal pdf*

2. The pdf of a sinusoid in noise [3 Bendat and Piersol, p. 37] is:

$$p(x) = \frac{1}{\sigma_n \pi \sqrt{2\pi}} \int_0^{\pi} e^{-\left(\frac{x - S\cos\theta}{4\sigma_n}\right)^2} d\theta \qquad \text{(A.2)}$$

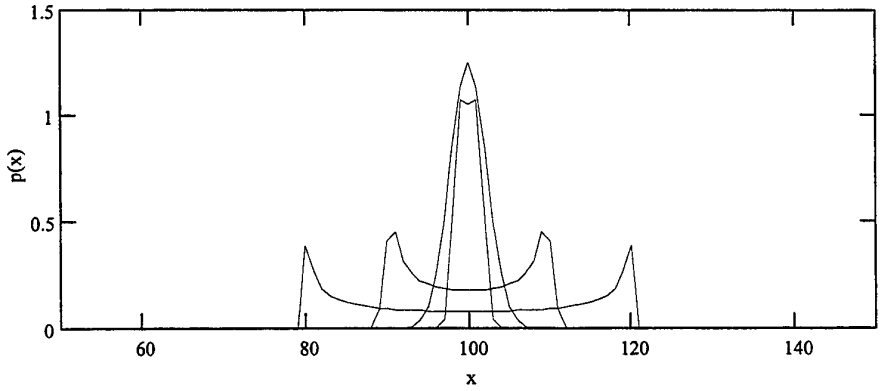


*Figure A.2 An example of a sinusoid in noise pdf*

Note how the shape transitions from a 'horned' to a flat peak and then a single peaked distribution as higher levels of noise are added to the sinusoid, corresponding to a reduction in the ratio $S/\sigma_n$, where $S$=amplitude of the sinusoid and $\sigma_n$=standard deviation of the Gaussian noise. Assumes zero mean for sinusoid and Gaussian noise.

3. The Gaussian pdf:

$$p(x) = \frac{1}{\sigma\sqrt{2\pi}} e^{-\frac{(x-\mu_x)^2}{2\sigma^2}} \qquad \text{(A.3)}$$

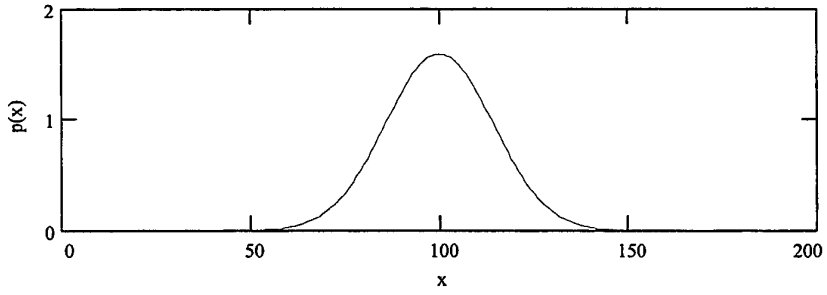


*Figure A.3 An example of the Gaussian function*

4. The Rayleigh pdf:

$$p(x) = \frac{x}{\sigma^2} e^{-\frac{x^2}{2\sigma^2}} \qquad \text{for } x \geq 0,\ p(x) = 0 \text{ otherwise} \qquad \text{(A.4)}$$

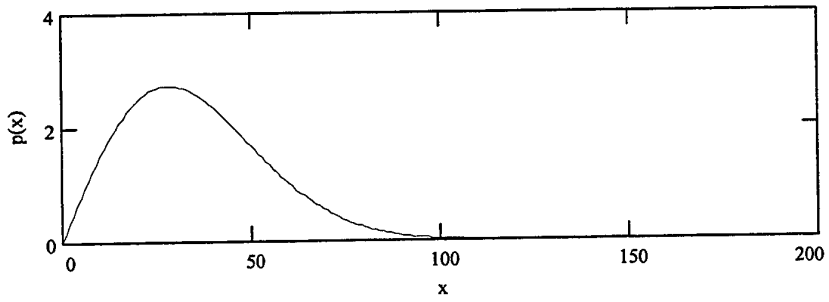


*Figure A.4 An example of the Rayleigh function*

5. The Rician pdf:

$$p(x) = \frac{x}{\sigma^2} e^{-\frac{x^2+A^2}{2\sigma^2}} I_0\left(\frac{Ax}{\sigma^2}\right) \qquad \text{for } x \geq 0,\ p(x) = 0 \text{ otherwise} \qquad \text{(A.5)}$$

where $I_0$ is the modified Bessel function of zero order defined by:

$$I_0(x) = \sum_{n=0}^{\infty} \frac{x^{2n}}{2^{2n}(n!)^2}$$

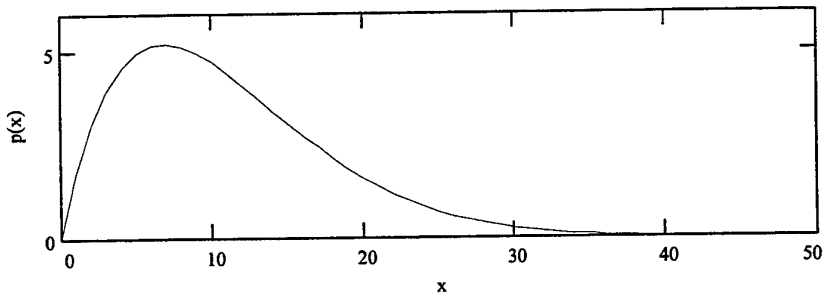


*Figure A.5 An example of the Rician function*

6. Chi-squared with $n$ degrees of freedom:

$$p(n,x) = \frac{x^{\frac{n}{2}-1}}{2^{\frac{n}{2}}\Gamma(\frac{n}{2})} e^{-\frac{x}{2}} \qquad \text{for } x > 0, \qquad p(n,x) = 0 \text{ otherwise} \qquad \text{(A.6)}$$

where $\Gamma$ is the Gamma function. Note the progressive resemblance to a Gaussian (or Normal) distribution with increasing $n$.

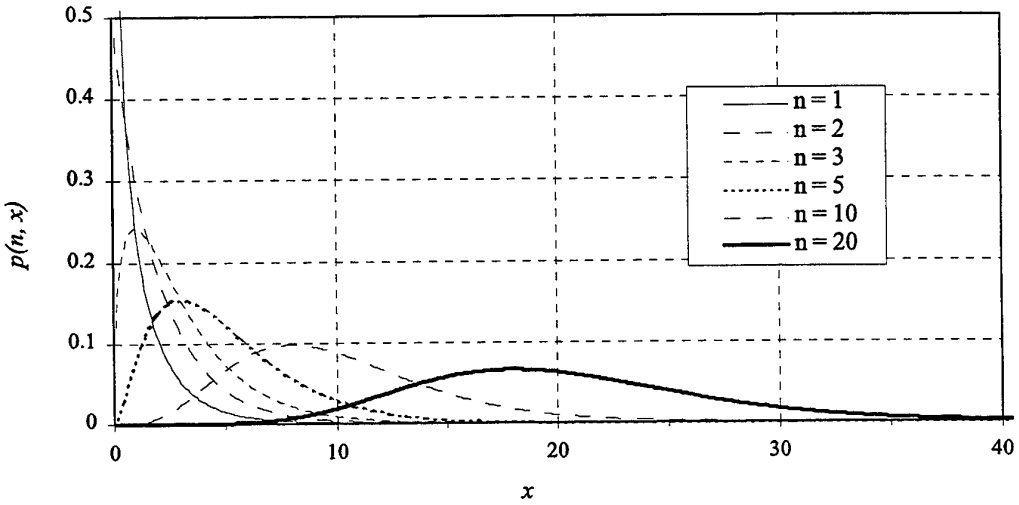


*Figure A.6 Examples of the $\chi^2$ function*

References.

1. Whalen, A. D. (1971) *Detection of Signals in Noise,* Academic Press, New York USA

2. Bendat, J. S. and Piersol, A. G. (1993) *Engineering Applications of Correlation and Sprectral Analysis,* second edition, John Wiley and Sons Inc. Canada

3. Bendat, J. S. and Piersol, A. G. (1993) *Random Data* second edition, John Wiley and Sons Inc. New York USA.

# Appendix B:
# Expressing Detection Index *d* in terms of $P_d$ and $P_{fa}$

Consider the probability density function of a noise source, $\phi_N$ and signal with noise, $\phi_{S+N}$ with means $M_N$ and $M_{S+N}$ respectively and common standard deviations $\sigma = \sigma_N = \sigma_{S+N}$. Figure A.1 illustrates the situation. See also [1 Nielsen, p.102].

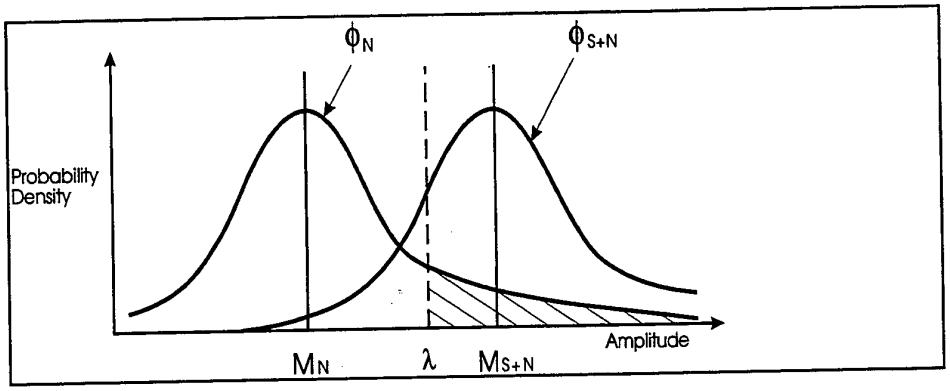


*Figure B.1 Noise and signal with noise probability density functions*

By definition [2 Urick, p.382], the detection index is the ratio:

$$d = \frac{[M_{S+N} - M_N]^2}{\sigma^2}$$

To illustrate how to obtain *d*, suppose $\phi_N$ and $\phi_{S+N}$ are Gaussian. Then the probability of a false alarm , $P_{fa}$ , is the probability of the noise alone exceeding a threshold amplitude $\lambda$, denoted by the shaded area in figure B.1:

$$P_{fa} = \int_{\lambda}^{\infty} \phi_N\left(\frac{x - M_N}{\sigma}\right) dx$$

$$= \int_{\frac{\lambda - M_N}{\sigma}}^{\infty} \phi(x)dx$$

$$\therefore P_{fa} = 1 - \Phi\left(\frac{\lambda - M_N}{\sigma}\right),$$

where $\Phi$ is the normalised cumulative Gaussian probability density function.

Now the detection probability, $P_d$, is the probability of the signal with noise source exceeding a threshold amplitude $\lambda$, and so similarly:

$$P_d = 1 - \Phi\left(\frac{\lambda - M_{S+N}}{\sigma}\right)$$

Rewriting the above two expressions yields:

$$\frac{\lambda - M_N}{\sigma} = \Phi^{-1}(1 - P_{fa}) \tag{B.1}$$

and

$$\frac{\lambda - M_{S+N}}{\sigma} = \Phi^{-1}(1 - P_d). \tag{B.2}$$

Recalling the definition of $d$ and taking the positive root,

$$\sqrt{d} = \frac{M_{S+N} - M_N}{\sigma} = \Phi^{-1}(1 - P_d) - \Phi^{-1}(1 - P_{fa})$$

Finally (B.1) - (B.2) gives:

$$\sqrt{d} = \frac{M_{S+N} - M_N}{\sigma} = \Phi^{-1}(1 - P_d) - \Phi^{-1}(1 - P_{fa}) \tag{B.3}$$

An ROC curve for the case of $P_d$=0.5 can be calculated from expression B.3, and this is shown in Figure B.2.

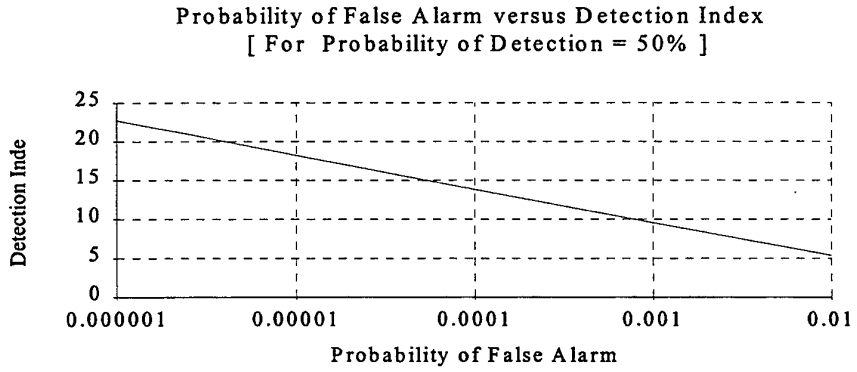


*Figure B.2 Detection Index d versus probability of false alarm $P_{fa}$*

References.

1. Nielsen, R. O. (1991) *Sonar Signal Processing*, Artech House, BostonUSA
2. Urick, R. J. (1983) *Principles of Underwater Sound* third edition, McGraw Hill, New York USA

# Appendix C:
# Nuttall Detection Threshold Correction to the Gaussian Approximation for Finite Bandwidth-Time Products for the case of a Sinusoid in Gaussian Noise

[1 Urick, figure 12.11] provides a family of curves which may be used to correct for the Gaussian approximation used in deriving an expression for *DT*, for the case of a band-limited Gaussian signal in Gaussian noise. These have been obtained from the analyses of [2 Nuttall and Magaraci] and [3 Nuttall and Garber]. The [1 Urick] text explains that slightly smaller *SNR* corrections would be required for the detection of sinusoidal signals in Gaussian noise. As precise estimates of performance are required, the correct curves for a sinusoid in Gaussian noise have been generated below.

From [3 Nuttall, figure 6], the required signal to noise ratio discrepancy between narrowband Gaussian and sinusoidal signals can be seen to be a maximum of about 1.5 dB for the two cases illustrated, with $P_d$=0.5. The discrepancy between sinewave signal detection and a Gaussian approximation is plotted here as Figure C.1, and is the difference between the dashed curve and points marked 'x' , for the given probabilities of false alarm, as a function of M=$wt$+1. Note that $w$ is identical to the $B$, and $t$ identical to the $T$ used in the main text.

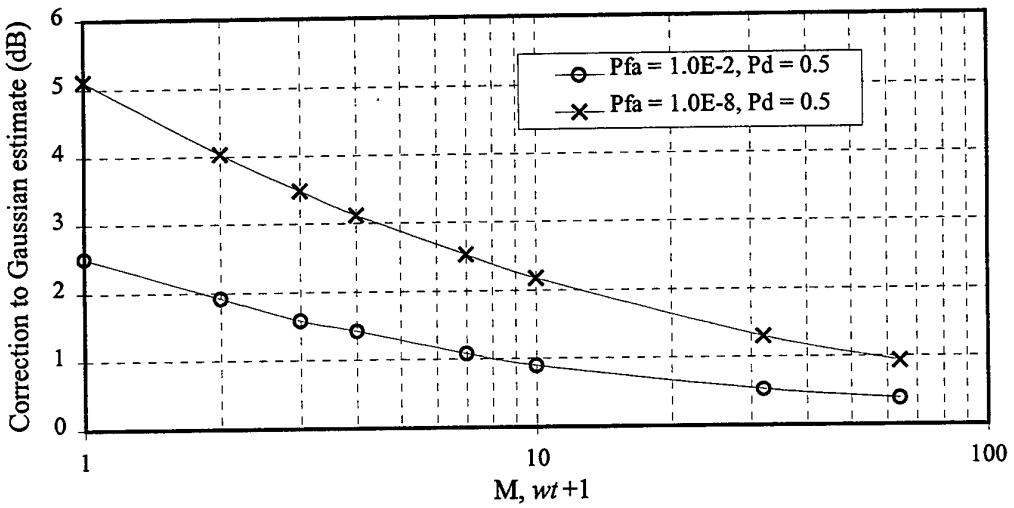


*Figure C.1 Finite wt+1 correction to Gaussian approximation of DT for power detection of a sinusoid in Gaussian noise, $P_{fa}$=$10^{-8}$ and $10^{-2}$ with $P_d$=50%.*

The curves above only apply to $P_{fa}$=$10^{-8}$ and $10^{-2}$; the more useful $P_{fa}$=$10^{-4}$ curve needs to be derived. This can be achieved from [2 Nuttall, figures 2 to 17]. With $P_d$=50%,

obtain $d_t$ from the plot off the corresponding figure. Then, by rearranging [3 Nuttall and Magaraci, equation 13],

$$\frac{S}{N} = \frac{d_t^2}{2(wt+1)} \tag{C.1}$$

where

$\frac{S}{N}$ = SNR = required signal to noise ratio
$w$ = narrowband filter bandwidth (Hertz)
$t$ = total integration time (seconds)

(Note: [3 Nuttall] refers to M= $wt$+1 = the number of independent squared envelope samples)

Now subtracting the required SNR above (in dB) from the Gaussian approximation value off [3 Nuttall, figure 6], a curve for the correction term for a given $P_{fa}$, as a function of $wt$+1, is obtained. Figure C.2 below was produced in this way. Note how the suggested curve fits are satisfactory for all but the M=1, $P_{fa}$=$10^{-8}$ point.

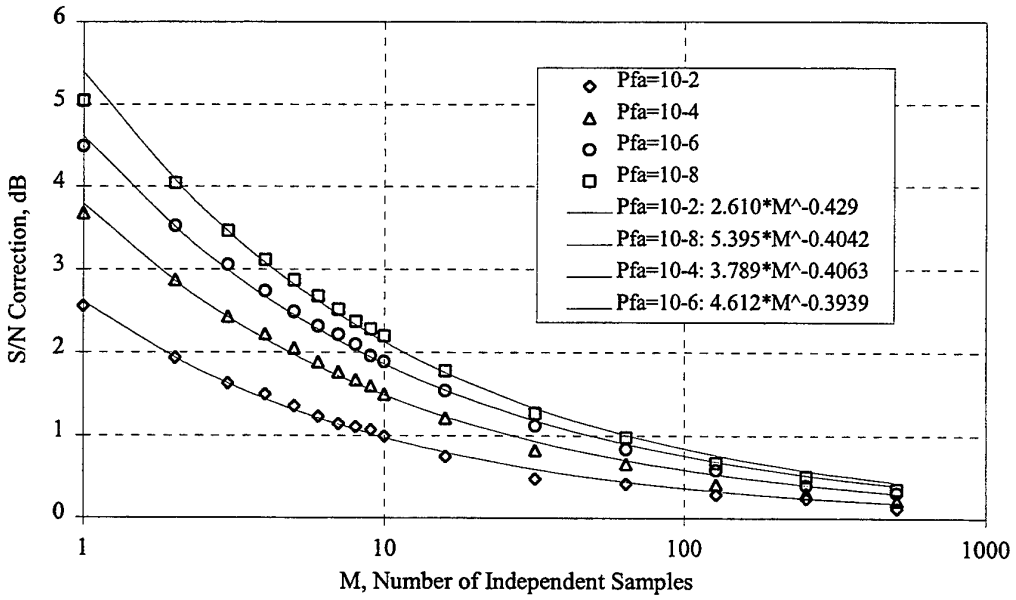


*Figure C.2 Finite wt+1 correction to Gaussian approximation of DT for power detection of a sinusoid in Gaussian noise, Pfa=$10^{-8}$, $10^{-6}$, $10^{-4}$ and $10^{-2}$ with Pd=50%, with curve fits.*

References.

1. Urick, R. J. (1983) *Principles of Underwater Sound* third edition, McGraw Hill, New York USA

2. Nuttall, A. H. and Garber, Robert. (28 September 1971) *Receiver Operating Characteristics for Phase-Incoherent Detection of Multiple Observations* NUSC Technical Memorandum No. TC-179-71

3. Nuttall, Albert. H. and Magaraci, Anthony F. (20 October 1972) *Signal-to-Noise Ratios Required for Short-Term Narrowband Detection of Gaussian Processes* NUSC Technical Report No. TR-4417

DISTRIBUTION LIST

Application of Detection Theory to the Measurement of the Minimum Detectable Signal for a Sinusoid in Gaussian Noise Displayed on a Lofargram

A. Grigorakis

**AUSTRALIA**

**DEFENCE ORGANISATION**

**Task Sponsor** Director of Naval Warfare

**S&T Program**

Chief Defence Scientist
FAS Science Policy } shared copy
AS Science Corporate Management
Director General Science Policy Development
Counsellor Defence Science, London (Doc Data Sheet )
Counsellor Defence Science, Washington (Doc Data Sheet )
Scientific Adviser to MRDC Thailand (Doc Data Sheet )
Director General Scientific Advisers and Trials/Scientific Adviser Policy and Command (shared copy)
Navy Scientific Adviser Scientific Adviser - Army (Doc Data Sheet and distribution list only)
Air Force Scientific Adviser
Director Trials

**Aeronautical and Maritime Research Laboratory**
Director

Chief of Maritime Operations Division
Research Leader, Sonar Technology & Processing
Head, ASW Sonar Systems
Head, Undersea Operations Research
Task Manager: C.J. Lightowler
J. Riley
L. Booth
L. Kelly
M. Swift
R. Dawe
J. Wang
E. Parker
M. Archer
S. Hoefs
S. Lourey
W. Elliston
J. Marwood
S. Taylor
A. Grigorakis

**DSTO Library**
Library Fishermens Bend
Library Maribyrnong
Library Salisbury (2 copies)
Australian Archives
Library, MOD, Pyrmont
Library, MOD, HMAS Stirling

**Capability Development Division**
Director General Maritime Development
Director General Land Development (Doc Data Sheet only)
Director General C3I Development (Doc Data Sheet only)

**Navy**
SO (Science), Director of Naval Warfare, Maritime Headquarters Annex, Garden Island, NSW 2000 (Doc Data Sheet only)

**Army**
ABCA Office, G-1-34, Russell Offices, Canberra (4 copies)
SO (Science), DJFHQ(L), MILPO Enoggera, Queensland 4051 (Doc Data Sheet only)
NAPOC QWG Engineer NBCD c/- DENGRS-A, HQ Engineer Centre Liverpool Military Area, NSW 2174 (Doc Data Sheet only)

**Air Force**
CO 292 Squadron RAAF Edinburgh

**Intelligence Program**
DGSTA Defence Intelligence Organisation
Library, Defence Signals Directorate (Doc Data Sheet only)

**Corporate Support Program (libraries)**
OIC TRS, Defence Regional Library, Canberra
Officer in Charge, Document Exchange Centre (DEC), 1 copy
*US Defence Technical Information Center, 2 copies
*UK Defence Research Information Centre, 2 copies
*Canada Defence Scientific Information Service, 1 copy
*NZ Defence Information Centre, 1 copy
National Library of Australia, 1 copy

**UNIVERSITIES AND COLLEGES**

Australian Defence Force Academy
Library
Head of Aerospace and Mechanical Engineering
Deakin University, Serials Section (M list), Deakin University Library, Geelong, 3217
Senior Librarian, Hargrave Library, Monash University
Librarian, Flinders University

**OTHER ORGANISATIONS**

NASA (Canberra)
AGPS

**OUTSIDE AUSTRALIA**

**ABSTRACTING AND INFORMATION ORGANISATIONS**

INSPEC: Acquisitions Section Institution of Electrical Engineers
Library, Chemical Abstracts Reference Service
Engineering Societies Library, US
Materials Information, Cambridge Scientific Abstracts, US
Documents Librarian, The Center for Research Libraries, US

**INFORMATION EXCHANGE AGREEMENT PARTNERS**

Acquisitions Unit, Science Reference and Information Service, UK
Library - Exchange Desk, National Institute of Standards and Technology, US

SPARES (10 copies)

**Total number of copies:** 75

**DEFENCE SCIENCE AND TECHNOLOGY ORGANISATION**
**DOCUMENT CONTROL DATA**

1. PRIVACY MARKING/CAVEAT (OF DOCUMENT)

2. TITLE

Application of Detection Theory to the Measurement of the Minimum Detectable Signal for a Sinusoid in Gaussian Noise Displayed on a Lofargram

3. SECURITY CLASSIFICATION (FOR UNCLASSIFIED REPORTS THAT ARE LIMITED RELEASE USE (L) NEXT TO DOCUMENT CLASSIFICATION)

| | |
|---|---|
| Document | (U) |
| Title | (U) |
| Abstract | (U) |

4. AUTHOR(S)

A. Grigorakis

5. CORPORATE AUTHOR

Aeronautical and Maritime Research Laboratory
PO Box 4331
Melbourne Vic 3001 Australia

| 6a. DSTO NUMBER | 6b. AR NUMBER | 6c. TYPE OF REPORT | 7. DOCUMENT DATE |
|---|---|---|---|
| DSTO-TR-0568 | AR-010-148 | Technical Report | August 1997 |

| 8. FILE NUMBER | 9. TASK NUMBER | 10. TASK SPONSOR | 11. NO. OF PAGES | 12. NO. OF REFERENCES |
|---|---|---|---|---|
| 510/207/0607 | ADA 95/161 | DGFDA | 41 | 41 |

13. DOWNGRADING/DELIMITING INSTRUCTIONS

None

14. RELEASE AUTHORITY

Chief, Maritime Operations Division

15. SECONDARY RELEASE STATEMENT OF THIS DOCUMENT

*Approved for public release*

OVERSEAS ENQUIRIES OUTSIDE STATED LIMITATIONS SHOULD BE REFERRED THROUGH DOCUMENT EXCHANGE CENTRE, DIS NETWORK OFFICE, DEPT OF DEFENCE, CAMPBELL PARK OFFICES, CANBERRA ACT 2600

16. DELIBERATE ANNOUNCEMENT

No Limitations

17. CASUAL ANNOUNCEMENT Yes

18. DEFTEST DESCRIPTORS

lofar, lofargram, detection threshold, minimum detectable signal, DT, MDS, detection theory

19. ABSTRACT

A review of detection threshold concepts is followed by an investigation into published theory for the detection of signals in noise. A set of empirical formulae relating minimum detectable signal to some basic sonar system parameters is presented. The formulae are compared and a recommendation made as to which is the most useful for the calculation of an omnidirectional narrowband lofargram minimum detectable signal for power detection of sinusoidal signals in Gaussian noise.